Theoretical and experimental studies about single cane reeds: a review

Amélie Gaillard, Vincent Koehl, Bruno Gazengel

Acta Acustica 2024, **8**, 63

https://doi.org/10.1051/aacus/2024050

Topical Issue – Musical Acoustics: Latest Advances in Analytical, Numerical and Experimental Methods Tackling Complex Phenomena in Musical Instruments

Available online at: https://acta-acustica.edpsciences.org

REVIEW ARTICLE OPEN ACCESS

Theoretical and experimental studies about single cane reeds: a review

Amélie Gaillard[1,2,*], Vincent Koehl[2], and Bruno Gazengel[1]

[1] Laboratoire d'Acoustique de l'Université du Mans (LAUM), UMR 6613, Institut d'Acoustique-Graduate School (IA-GS), CNRS, Le Mans Université, Avenue O. Messiaen, Cedex 09, 72085 Le Mans, France
[2] Univ Brest, CNRS, Lab-STICC, 6 avenue Victor Le Gorgeu, 29200 Brest, France

Received 7 March 2024, Accepted 6 August 2024

Abstract – Since the late 19th century, researchers have measured and predicted the acoustic properties of single-reed instruments like the clarinet and saxophone. According to musicians, the reed itself has a significant impact on sound production and playing comfort. However, the physics of the reed remains incompletely understood, and reed makers are constantly seeking a deeper comprehension that could allow them to deduce physical parameters that more adequately account for the sensations of musicians. This is the reason why some researchers are interested in studying the behavior of reeds, either through the creation of physical models or through physical or perceptual experiments. The present paper proposes a review of these studies, structured into three sections. Firstly, the physics of single-reeds and single-reed instruments is exposed and described by various models of increasing complexity. The experimental studies about single cane reeds are then detailed in the second and third sections, which respectively deal with perceptual assessments and physical measurements. Finally, the conclusion synthesizes and brings together the findings from each section to provide a comprehensive overview of current knowledge while also highlighting prospects for future research.

Keywords: Single cane reeds, Woodwinds, Theoretical models, Perceptual assessments, Physical measurements

List of symbols

Latin

$A(x)$	Reed cross section at position x (m^2)
A_r	Reed equivalent area (m^2)
$b(x)$	Reed thickness at position x (m)
c	Speed of sound (m s^{-1})
C_c	Contraction coefficient (–)
E'	Dynamic reed material Young's modulus (N m^{-2})
E_x	Longitudinal reed material Young's modulus (N m^{-2})
E_y	Transverse reed material Young's modulus (N m^{-2})
$F(x)$	Force per unit length due to the pressure difference across the reed (N m^{-1})
F_0	Static lip force ($F = F_0$ for $\Delta p = 0$) (N)
F_c	Contact force from Hunt-Crossley impact model (N)
G_{xy}	Reed material shear modulus in plane xy (N m^{-2})
G_{xz}	Reed material shear modulus in plane xz (N m^{-2})
G_{yz}	Reed material shear modulus in plane yz (N m^{-2})
$h(x)$	Reed displacement at position x (m)
h	Reed channel height (m)
h_0	Reed channel height at rest with static force F_0 (m)
h_c	Reed displacement value below which the nonlinear stiffness exists (m)
h_e	Effective reed channel height (m)
h_r	Dimensionless reed channel height (–)
h_{00}	Reed channel height at rest with no static force (m)
$I(x)$	Quadratic moment of the reed at position x (m^4)
K_a	Reed equivalent stiffness per unit area (N m^{-3})
K_c	Reed nonlinear stiffness parameter (N m^{-4})
K_m	Reed mechanical stiffness (N m^{-1})
K_p	Reed point stiffness (N m^{-1})
K_r	Reed equivalent stiffness (N m^{-1})
l	Reed channel length (m)
l_r	Length of jet reattachement (m)
M_a	Reed equivalent mass per unit area (kg m^{-2})
M_r	Reed equivalent mass (kg)
p	Mouthpiece pressure (Pa)
P_M	Static reed closure pressure (Pa)
P_m	Mouth pressure (Pa)
P_{Th}	Threshold pressure (Pa)

*Corresponding author: amelie.gaillard@univ-lemans.fr

Q_r	Reed quality factor (–)
q_r	Reed damping coefficient, inverse of quality factor (–)
R_a	Reed equivalent damping per unit area (kg s^{-1} m^{-2})
R_r	Reed equivalent damping (kg s^{-1})
R_{ul}	Reed damping per unit length (kg s^{-1} m^{-1})
S	Cross section of the resonator (m^2)
S_d	Reed driving surface (m^2)
S_e	Effective reed channel opening section (m^2)
S_f	Front reed channel opening section (m^2)
S_r	Reed flow-related effective surface (m^2)
S_s	Side reed channel opening section (m^2)
S_{op}	Total reed channel opening section (m^2)
U	Volume flow entering the resonator (m^3 s^{-1})
U_c	Volume flow in the reed channel (m^3 s^{-1})
U_r	Volume flow induced by the reed (m^3 s^{-1})
V_{eq}	Equivalent volume of reed (m^3)
w	Reed channel width (m)
x	Longitudinal position on reed (m)
$y(x)$	Vertical displacement of the reed at position x (m)

Greek

α	Power law constant for nonlinear stiffness (–)
β	Damping coefficient in the Hunt-Crossley impact model (s m^{-1})
Δl	Equivalent correction length of reed (m)
$\Delta p = P_m - p$	Pressure drop across the reed channel (Pa)
Δp_g	Generalized pressure drop across the reed channel (Pa)
δ	Damping of the fluid surrounding the reed (–)
η_r	Magnitude of the internal reed viscoelastic losses (–)
γ	Relative mouth pressure(–)
ν_x	Reed material Poisson's ratio when a stress is applied in the x direction (–)
ν_y	Reed material Poisson's ratio when a stress is applied in the y direction (–)
ω_r	Reed angular resonance frequency (s^{-1})
ρ	Air density (kg m^{-3})
ρ_r	Reed material density (kg m^{-3})
ζ	Embouchure parameter or dimensionless reed opening parameter (–)

1 Introduction

A wind instrument or aerophone is a musical instrument supplied by a source of air. It includes woodwind, brass and free-reed instruments. Free-reed instruments such as the accordion use a source of pressure and the sound is generated by the coupling between an air jet and the reed. In these instruments the playing frequency is mainly controlled by the reed properties [1]. In brass and woodwind instruments, a column of air is set into vibration thanks to the energy supplied by the player. For brass instruments, the source of energy is the pressure in the player's mouth and the sound is generated thanks to the coupling between the air column and the player's lip. In this case, the player controls the resonance frequency of the lips and the playing frequency is determined mainly by the air column but can also be controlled by the lip resonance frequency [2]. For woodwinds instruments the source of energy is divided into two families. On the one hand, instruments can produce a sound thanks to an air-jet which oscillates due to the coupling between the jet and the air column (flutes). On the other hand, single or double reed instruments produce a sound thanks to a constant pressure converted into acoustic pressure due to coupling between the air column and the reed which creates a pulsating flow in the instrument. For these instruments, the source of pressure can be located in the mouth of the player (clarinet, saxophone, oboe, bassoon) or in an air pocket (bagpipes). The present paper focuses on single reeds. They appear to have a small impact on the pitch compared to free reeds or lips (for brass instruments) but they can largely affect other playing parameters such as ease of playing, timbre and clean intonation [3].

Single reeds are usually made from a grassy plant designated as *Arundo donax* L. according to the Linnaean binomial nomenclature [4, 5]. It is mainly grown in the French region of *Provence* due to the optimal climatic environment [6]. For this reason, it is more commonly known as *Canne de Provence*. The process of making a reed, from plant to sale, takes time and requires high-precision tools. Once the two-year canes have been harvested, they undergo a drying process first in the sun and then in a warehouse for at least two years. When the stems are completely dry, the plant can be shaped into reeds. Firstly, the canes are cut so that only hollow tubes remain, and the knots are removed. The tubes are split lengthways into four quarters to form four reeds. Each quarter is cleaned and then the inside surface is flattened. The outer surface of the sample undergoes several stages of planing until it has the desired cut (i.e. geometry). The thin extremity is then rounded [7–9] as depicted in Figure 1. Finally, each reed is submitted to a flexibility test to be graded on a scale describing its strength usually from one (very soft) to five (very strong) [10]. Reeds are distinguished by three main characteristics: cut, strength and brand. For a musician, the choice of reed strength is partly conditioned by the type of mouthpiece used, especially with respect to the tip opening.

Until the industrialization of the reed-making process at the end of the nineteenth century, each musician made his own reeds by hand [7, 12, 13]. It was therefore difficult to cut all the reeds identically, which could explain quality disparities. Nowadays, despite the very precise automated manufacturing process, the perceived quality is still not uniform among reeds. According to a survey of clarinetists and saxophonists around the world [14, 15], only 30% of reeds are of very good quality. The rest are of average (40%) or even mediocre (30%) quality. Manufacturers are still struggling to understand and predict these differences. Some tried to overcome this issue by designing new synthetic materials to produce reeds with exact same physical

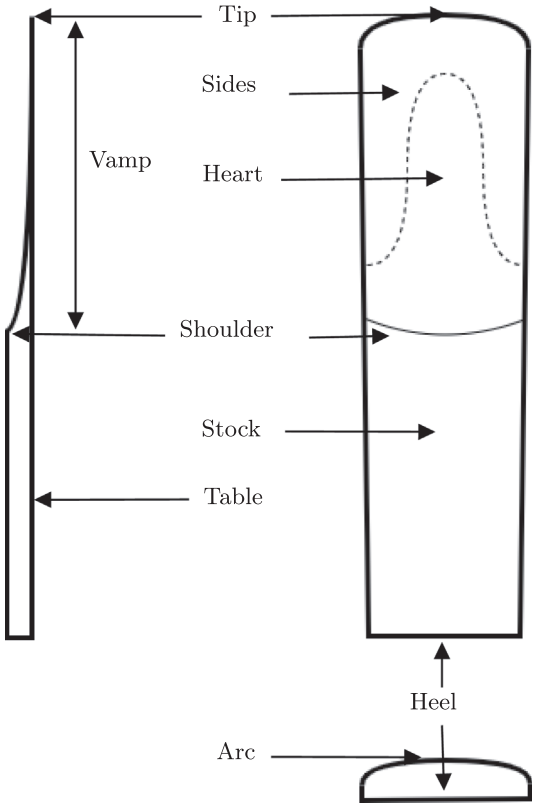

Figure 1. Reed sketch inspired from Intravaia and Resnick [11].

properties [16] and to finally replace natural cane. Although this sounds promising, the vast majority of musicians still prefer traditional cane to synthetic reeds.

The current paper proposes an overview of the current knowledge about single cane reeds. Despite the numerous studies that are cited throughout this review, there is still way to go to fully understand the reed behavior in playing situation. As an example, the relationships between physical models and experimental results (both perceptual and physical) are not thoroughly described so far. Such issues specific to single reeds are not addressed in depth by the current reference books about musical instruments [17, 18] or even more precisely about wind instruments [2, 8].

This paper is structured in three sections. Section 2 presents the different physical models used to describe the behavior of the reed itself or the behavior of the exciter (reed, mouthpiece, player's lip). It introduces several model parameters that enable to better understand the role of the reed on the self-sustained oscillations or that can be used for simulations. These models also give information on which physical quantity should be measured to characterize reeds. The two following Sections 3 and 4 are devoted to experimental researches on reeds. Section 3 describes the different perceptual assessments conducted on clarinet or saxophone reeds with musicians. Section 4 lists the numerous experimental approaches designed to understand the reed behavior and estimate reed parameters values. A list of numerical values extracted from this section is given in Appendices A–C. To conclude, the relationships between perceptual and physical characterization are explored and future works are discussed.

2 Physics of single reed instruments

Single cane reed instruments are self-oscillating systems. The steady-state energy of the source (provided by the pressure in the musician's mouth) is converted into self-sustained oscillations in the instrument thanks to the mutual coupling between the resonator and a nonlinear system localized in the exciter (composed of the mouthpiece and the reed [19]). In this system, the reed acts as a pressure-controlled valve [17, 20] whose main role is to close and open the reed channel defined in Figure 2. This modifies the reed opening section and consequently the volume flow velocity entering the resonator.

While playing, the musician controls the mouth pressure, the lip force acting on the reed (which controls the opening section of the reed channel at rest) and the lip position along the length of the reed. These parameters are assumed to vary slowly over time compared to the pressure variations in the mouthpiece. The player can also control the reed channel opening with his tongue in order to control the transient characteristics [21, 22].

The physical variables involved in this system are presented in Figure 2. They are the mouth pressure P_m, the mouthpiece pressure p, the volume flow in the reed channel U_c, the volume flow entering the resonator U. The reed channel height is written h. The channel height at rest is h_0 when the player applies the static force F_0 on the reed. The channel height can also be described as a dimensionless variable $h_r = \frac{h}{h_0}$ [23]. Depending on the studies, the reed at rest with a lip force F_0 can be defined by $h = 0$ [24, 25] or $h = h_0$ [26]. The closing of the reed on the mouthpiece can occur for $h = 0$ (see Fig. 2) [26], $h = h_0$ ($h_r = 1$) [24] or $h = -h_0$ ($h_r = -1$) [25]. The volume flow produced by the reed movement is written $U_r = S_r\dot{h}$ where S_r is the flow-related effective surface.

The mechanical properties of the reed can be described by local parameters (density ρ_r, Young's moduli E_x, E_y, shear moduli G_{xy}, G_{xz}, G_{yz}, Poisson's ratio ν_x, ν_y) [27], or global parameters when the reed is modeled as a system with one degree of freedom. In the later case, they are the mass M_r (kg), the damping R_r (kg s^{-1}), the stiffness K_r (N m^{-1}), and the driving surface S_d (m^2) [28]. Parameters per unit area, also called effective parameters are used in some papers ($M_a = \frac{M_r}{S_d}$, $R_a = \frac{R_r}{S_d}$, $K_a = \frac{K_r}{S_d}$) [24]. Lastly, some authors [29] characterize the reed mechanics using the damping coefficient $q_r = \frac{\omega_r R_r}{K_r}$ (inverse of quality factor) and the resonance angular frequency $\omega_r = \sqrt{\frac{K_r}{M_r}}$. These authors also describe the reed opening with the dimensionless channel height h_r.

The reed has been studied by several researchers and has been considered as a system with different degrees of complexity, starting from a simple spring and going to a two-dimensional system with complex boundary conditions (mouthpiece and lip). Figure 3 shows the reed models

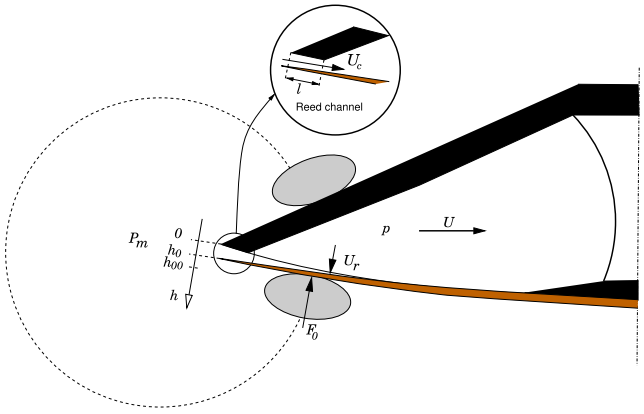

Figure 2. View of the exciter and definition of the physical variables used in the model of the instrument.

presented in the following sections and gives a list of the references used in this paper.

2.1 Elementary model for single reed instruments

This section presents the elementary model describing the instrument and enabling to explain the production of self-sustained oscillations. In this model, the reed is assumed to behave as an ideal spring characterized by its effective stiffness K_a (in Pa m^{-1}) [31].

2.1.1 Resonator

The resonator is composed of the instrument bore and of the mouthpiece. It is usually characterized by its input impedance at low-level acoustic pressures, assuming linear behavior. The impedance Z is defined in the frequency domain by

$$Z(\omega) = \frac{p(\omega)}{U(\omega)}, \tag{1}$$

where ω is the angular frequency.

2.1.2 Flow entering the exciter

The flow entering the exciter is controlled by the reed channel height $h(t)$ and by the pressure drop between the mouth and the mouthpiece $\Delta p(t) = P_{\mathrm{m}} - p(t)$. Assuming a quasi-stationary behavior and a very short reed channel ($l/h \leq 1$ with l the channel length defined in Fig. 2), Hirschberg et al. [30] showed that the air passes through the channel and that a jet is created in the mouthpiece after the flow separation from the walls. For high ratios ($l/h \geq 3$), the jet reattaches at a fixed point $l_r \simeq h$ measured from the channel's entrance. In the case of short channels, the flow can be modeled by the Bernoulli theorem, taking into account a contraction coefficient [26].

Assuming that the reed channel is a rectangle aperture of width w and height $h(t)$, the volume velocity U_c in the reed channel is written

$$U_c(t) = wh_e(t) \cdot \mathrm{sign}[\Delta p(t)] \cdot \sqrt{\frac{2|\Delta p(t)|}{\rho}}, \tag{2}$$

with $h_e(t) = C_c h(t)$ the effective reed opening, taking into account the contraction coefficient C_c. The effective opening section $S_e(t) = wh_e(t)$ is different from the front opening of the reed channel $S_f(t) = wh(t)$ not only because of the contraction coefficient but also because the air can enter through the lateral cross-section, which implies considering the effect of lateral flow. Chatziioannou [48] defined the effective opening section as $S_e = C_c^{\exp} S_{op}$, with $C_c^{\exp}$ the experimental contraction coefficient. S_{op} is the total opening surface of the reed, defined as $S_{op} = 0.69\,(S_f + S_s)$, with S_f the front opening surface and S_s the side opening surfaces, as suggested by experimental data [53] and also discussed by Yoshinaga et al. [54] or Taillard [55].

As demonstrated by Chatziioannou [48], in the quasi-static configuration, the experimental contraction coefficient $C_c^{\exp}$ is dependent upon the reed opening $h(t)$, and for $h > 0.3$ mm for the clarinet, $C_c^{\exp} \simeq 0.85$ (refer to Fig. 4.8 in the reference [48]).

It should also be noticed that the quasi-stationary model in equation (2) is not valid in the dynamic case, as shown by Ricardo da Silva et al. [46] using Lattice-Boltzmann simulation.

2.1.3 Nonlinear characteristics

Assuming that the reed behaves as an ideal spring with stiffness K_a leads to

$$h(t) = \begin{cases} h_0 - \dfrac{\Delta p(t)}{K_a} & \text{if } \Delta p(t) \leq P_M, \\ 0 & \text{if } \Delta p(t) \geq P_M, \end{cases} \tag{3}$$

where h_0 is the reed opening at rest due to the static lip force F_0 and $P_M = K_a h_0$ is the static reed channel closure pressure (lowest pressure value for which the reed channel is closed). According to results obtained by Gazengel et al. [32], h_0 can be written

$$h_0 = h_{00} - \frac{F_0}{K_m}, \tag{4}$$

where h_{00} is the opening at rest with no lip force ($F_0 = 0$), and K_m is the mechanical stiffness of the reed, defined as $K_m = K_a A_r$. The reed equivalent area, A_r, can be defined by considering the mouth pressure Δp_0 with no lip force or the static lip force F_0 with no mouth pressure. Assuming that F_0 and Δp_0 result in the same reed tip displacement h_0, the reed equivalent area is written as $A_r = \frac{F_0}{\Delta p_0}$, meaning that both effects (force and pressure) are equivalent.

$$U_c(t) = \begin{cases} U_A \cdot \mathrm{sign}[\Delta p(t)] \cdot \left(1 - \dfrac{\Delta p(t)}{P_M}\right) \cdot \sqrt{\dfrac{|\Delta p(t)|}{P_M}}, & \text{if } \Delta p(t) \leq K_a h_0 \\ 0 & \text{if } \Delta p(t) \geq K_a h_0 \end{cases} \tag{5}$$

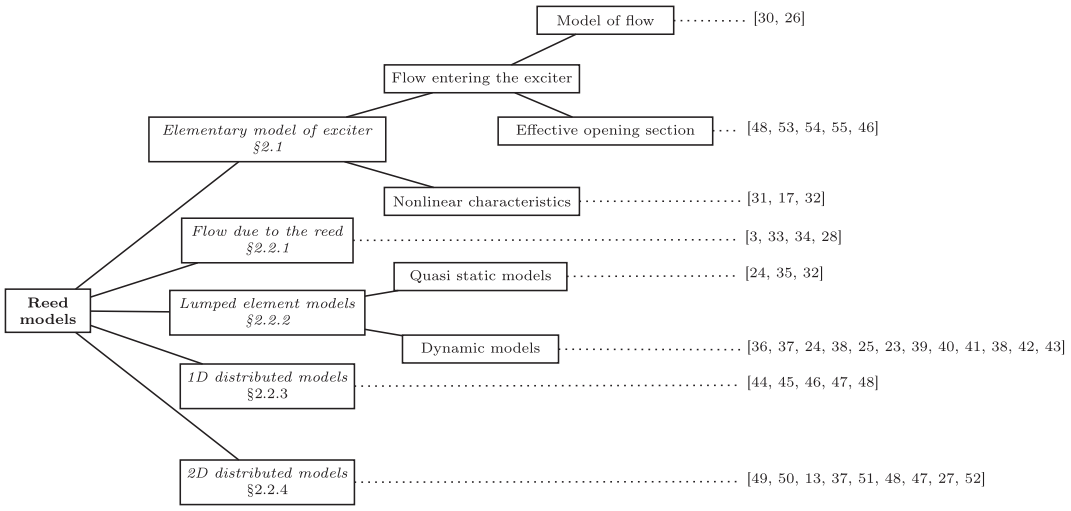

Figure 3. List of literature references presented in this paper and dedicated to the study of the single cane reed.

Combining equations (2), (3) and (4) leads to

See the Equation (5) bottom of previous page

where $U_A = wC_c h_0 \sqrt{\frac{2K_a h_0}{\rho}}$. U_A is a volume velocity amplitude parameter that depends on the reed effective stiffness K_a, on the reed opening at rest h_0 (which depends on h_{00}, on the lip force F_0, and on the reed mechanical stiffness K_m). The volume velocity U_c is plotted in Figure 4 as a function of Δp for three different force values. In Figure 4, $P_{M0} = K_a h_{00}$, $U_{A0} = C_c w h_{00} \sqrt{\frac{2P_{M0}}{\rho}}$ and $F_M = K_m h_{00}$.

The volume flow U_c shows a maximum $U_{\max} = \frac{2}{3\sqrt{3}} U_A$ for $\Delta p = \frac{1}{3} P_M$ which depends on lip force F_0. After this maximum, the flow decreases and the reed channel closes completely for $\Delta p = P_M$. In the increasing part of the curve ($\Delta p \leq \frac{P_M}{3}$), the conductance of the system (obtained as the first derivative) is positive, meaning that the exciter acts as a resistance to the air flow. However, in the decreasing part of the curve ($\Delta p \geq \frac{P_M}{3}$), the conductance is negative and the exciter acts as an acoustic generator. Thus, the generation

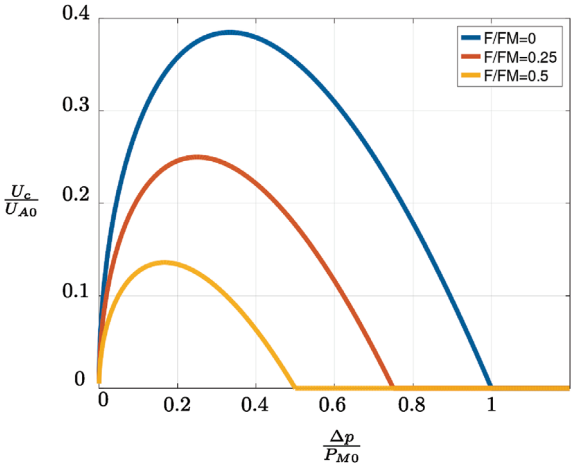

Figure 4. Volume flow as a function of the pressure difference across the reed.

of self-sustained oscillations is possible [17]. As a result, the threshold pressure for the beginning of the self-sustained oscillations is $\frac{1}{3} P_M$, ignoring losses in the resonator [31].

2.2 Physical models of the reed

The simple model given by equations (1) and (5) enables to get self-sustained oscillations thanks to a resonator coupled with an exciter showing a nonlinear behavior. This exciter controls the volume flow entering the mouthpiece thanks to a reed acting as a spring and closing the reed channel, assuming an inelastic collision. The threshold pressure of the oscillations is determined by the reed effective stiffness K_a and by the opening at rest $h_0 = h_{00} - \frac{F_0}{K_m}$. This model shows that the reed parameters K_a and h_0 (depending on h_{00} and K_m) are of major importance in the functioning of a woodwind instrument.

However, the reed is in contact with the lip, the mouthpiece lay and sometimes the tongue. In a quasi-static regime, the mouthpiece lay has an impact on the reed stiffness, creating a nonlinear effect (an increase in stiffness when the reed closes). In the dynamic regime, the damping provided by the lips of the player enables to damp the reed resonance and to prevent the apparition of a squeak. By moving the lower lip along the reed, the player can adjust this damping as well as the effective mass and stiffness of the reed. However, the reed dynamic is more complex at high sound levels when the reed starts to interact with the mouthpiece lay (reed beating). In order to describe these complex effects, different physical models of the reed have been proposed in the literature and are discussed in the following subsections. These models are presented in order of increasing complexity.

2.2.1 Flow due to the reed

While vibrating, the reed produces an air flow $U_r(t) = S_r \dot{h}(t)$ induced by its flow-related surface S_r so that the total incoming volume flow in the instrument is $U(t) = U_c(t) - U_r(t)$. Nederveen [56] and Dalmont et al.

[33] demonstrated that this reed flow can be understood as a correction length applied to the resonator in the case of a non-beating reed ($h(t) < h_0$). This correction length can be written as $\Delta l = \frac{\rho c^2}{K_a}\frac{S_r}{S}$, with ρ the air density, c the sound speed, and S the cross-section of the resonator. It can be explained as the effect of the compliance of the reed acting as a supplementary volume of air at the resonator entry. Dalmont et al. [3] reported typical clarinet correction lengths of 10 mm. Nederveen [57] related Δl to the reed strength and showed that Δl may approximately vary from 6 mm (strong reeds) to 9 mm (softer reeds).

According to Dalmont et al. [33], when the reed is beating, its equivalent volume V_{eq} is determined by the mouthpiece pressure p. This can be expressed as follows: $V_{eq} = \frac{\rho c^2 S_r h_0}{2|p|}$. This indicates that the reed's playing frequency tends to increase as the amplitude of the sound. Numerical simulations demonstrating that the decrease in the flow rate effect is the cause of the increase in playing frequency above the beating reed threshold [34] corroborate this conclusion. However, for high mouth pressure values, the analytical model overestimates the predicted frequency compared to numerical simulations.

Section S_r can be derived knowing the reed deflection along its length. Considering the potential energy of the reed, van Walstijn and Avanzini [28] showed that the driving surface S_d and the flow-related surface S_r are identical.

2.2.2 Lumped element models

The model of reed presented in Section 2.1.3 considers the reed as a pure spring. This assumption does not consider dynamic effects due to the lip (damping) and the reed inertia (mass), nor does it consider the variation of stiffness when the reed bends on the mouthpiece rails. Lumped element models considering these effects have been proposed in the literature and are presented below.

Quasi static models

The effect of bending the reed on the lay of the mouthpiece was modelled by Chatziioannou and van Walstijn [24] as a conditional contact force, written in the form of a power law[1]. This nonlinear part is added to the linear stiffness K_a to write a nonlinear spring model as follows:

$$K_a(h - h_0) - K_c(\lfloor h_c - h \rfloor)^{\alpha} = -\Delta p, \tag{6}$$

where K_c is the nonlinear stiffness parameter and α is a power-law constant. The nonlinear part is written

$$\lfloor h_c - h \rfloor = \begin{cases} h_c - h & if \quad h < h_c, \\ 0 & if \quad h \geq h_c. \end{cases} \tag{7}$$

In equation (7), h_c is the displacement value below which the power law becomes active. For $\alpha = 2$, the nonlinear stiffness provided by equation (6) and shown in Figure 5 fits the stiffness obtained from a distributed model [35]. The limitation of this model is that the reed tip displacement h is not asymptotically close to 0 (or to h_0 in [24]) so that the reed penetrates into the mouthpiece. The simplest linear model (eq. (3)) explains this closing (see Fig. 5) but does not take into account the bending of the reed on the mouthpiece lay.

[1] This model is written with different variables from those used in this review. In the work of Chatziioannou and van Walstijn [24], the reed tip opening is written y. In this work, it is written $h_0 - h$ so that the equivalence between the two models is $y = h_0 - h$.

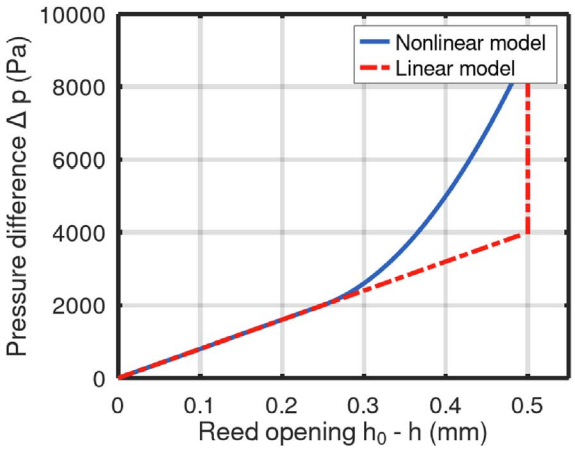

Figure 5. Pressure difference Δp versus reed tip displacement $h_0 - h$, for $h_0 = 0.5$. The solid curve (nonlinear model, Eq. (7)) is obtained with $K_a = 8000$, $K_c = 80000$, $h_0 - h_c = 0.25$. The dashed curve shows the linear model (Eq. (3)).

According to a different model, the reed effective opening section S_e (defined in Sect. 2.1.2) is a piece-wise function of the pressure drop Δp or of the generalized pressure $\Delta p_g = \Delta p + F/A_r$, where F is the lip force and A_r the lip's effective area. This model assumes that the effect of bending on the mouthpiece is represented by a parabola (for $N = 3$ [32]) or a set of parabola (for $N > 3$ [55]) and can also take into account the effect of residual leakage (Fig. 6) which can be due to a bad contact between the reed tip and the mouthpiece.

Dynamic models

More often, the reed is modeled as a one degree of freedom system in order to consider the effective mass M_a and damping R_a (mainly caused by the lip). In these models, the effect of mouthpiece lay and tongue are written as variable stiffness and sometimes as variable mass and damping terms.

Ducasse [36] proposed to consider the reed parameters as functions of the reed position written as follows:

$$M_a(h) \cdot \ddot{h} + \left[\frac{\mathrm{d}M_a}{\mathrm{d}h} \cdot \dot{h} + R_a(h)\right] \cdot \dot{h} + K_a(h) \cdot (h - h_0) = -\Delta p. \tag{8}$$

In this model, the parameters $K_a(h)$ and $M_a(h)$ are primarily related to the reed density and longitudinal flexibility and they also depend on the geometry of both the reed and the mouthpiece, taking into account the bending of the reed on the lay of the mouthpiece. The damping $R_a(h)$ is considered to be mainly produced by the lip, so that the reed is considered a highly-damped reed. The variability of the parameters according to h is in particular used to

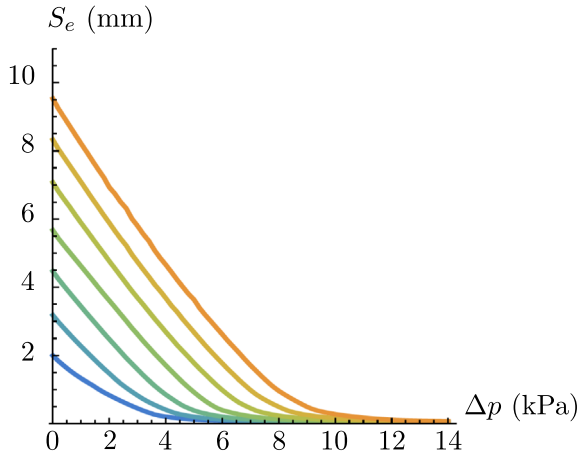

Figure 6. Reed effective opening section S_e as a function of pressure drop Δp for 7 different lip positions [55]. The 7 lip positions along the z-axis defined in Figure A1 are encoded by the colors from orange to blue with decreasing z.

take into account the bending of the reed on the mouthpiece lay. This bending occurs when the reed tip position h is smaller than a limit h_c. It is modeled using a constant damping term, a nonlinear stiffness proportional to $h_c - h$ and a nonlinear mass proportional to $(h_c - h)^2$. Analytical expressions of the effective reed parameters are given in Ducasse's thesis [37] (Appendix, p. 97). Ducasse modeled the tongue as another mass-spring system which can touch the reed as a perfectly soft shock.

More recently, the mouthpiece-reed contact has been modeled taking into account a separate contact force consisting of a stiffness term and a damping term (Hunt-Crossley impact model [39]). The contact force is activated when the reed is in contact with the mouthpiece for a specific channel height h_c. It is due to the contact between the reed and the mouthpiece when the reed curvature is higher than the mouthpiece lay curvature [25, 47]. As the contact force is activated for $h \leq h_c$, the reed movement is described by

$$M_a \cdot \ddot{h} + R_a \cdot \dot{h} + K_a \cdot (h - h_0) = -\Delta p + \frac{F_c}{S_d}, \qquad (9)$$

where S_d is the driving area and F_c the contact force defined by

$$\frac{F_c}{S_d} = K_c(\lfloor h_c - h \rfloor)^{\alpha}(1 - \beta \dot{h}). \qquad (10)$$

The term $\lfloor h_c - h \rfloor = \frac{h_c - h + |h_c - h|}{2} = \max(h_c - h, 0)$, also defined in equation (7), is the ramp function. K_c is the nonlinear stiffness parameter, $\alpha \geq 1$ a power law exponent, and β a damping coefficient. α is typically set to 2 to describe the interaction between the reed and the mouthpiece lay, resulting in a quadratic stiffness activated when the reed meets the lay at height h_c. The ramp function can be regularized using a parameter η (chosen equal to 10^{-3}) to avoid non-differentiability at $h = h_c$ (reed contact) by writing $\frac{h_c - h + |h_c - h|}{2} \simeq \frac{h_c - h + \sqrt{(h_c - h)^2 + \eta}}{2}$ [23]. Alternatively, the activation of the contact force can be considered when the reed tip is contact with the mouthpiece ($h = 0$) and not for $h = h_c$. Finally, some authors [40, 41] consider the "phantom reed" or "ghost reed" model, assuming that $F_c = 0$ but that the volume velocity U_c vanishes when the reed closes.

Considering the contact force with no damping term, Chatziioannou and Hofmann [38] modeled the reed as a spring mass system with effective stiffness K_a depending on reed tip position:

$$M_a \cdot \ddot{h} + R_a \cdot \dot{h} + K_a \cdot (h - h_0) - K_c \cdot (\lfloor h_c - h \rfloor)^{\alpha} = -\Delta p, \qquad (11)$$

where $\lfloor h_c - h \rfloor$ is defined in equation (7). They included the effect of mouthpiece lay and the action of the tongue by varying the parameters $M_a(h)$, $R_a(h)$ and h_0 in the attacks. They used this description to compare tongue-separated tones and pressure-separated tones. Muñoz Arancón et al. [42] studied the efficiency of this model. They showed that for low playing levels (up to piano nuance) and without considering the tongue effect, the reed can be modeled by using a nonlinear stiffness term $K_a(h)$ and a constant damping term R_a, which validates the model given in equation (11) without considering the effect of mass. For *mezzo forte* nuance, the model fits the measurement, but the shock of the reed on the mouthpiece is not well explained. For higher playing level (*forte* nuance), this model is no longer valid.

More recently Chatziioannou et al. [43] considered constant terms for mass and damping. They introduced nonlinear terms for modeling the reed mouthpiece collision and the tongue reed interaction using contact forces depending on the contact stiffness K_κ, contact position h_κ, collision exponent α_κ, contact damping β_κ, κ describing either the reed-mouthpiece collision or the tongue-reed interaction.

2.2.3 One-dimensional distributed models

Instead of modeling the reed using lumped elements, some authors chose to suggest a more realistic model, based on the idea that the reed can be understood as a homogeneous, isotropic, cantilevered beam with variable cross-sections, where the tip is thinner than the shoulder. According to this theory, the vertical displacement $y(x, t)$ of a non- uniform clamped beam with width w and thickness $b(x)$ is determined by:

$$\rho_r A(x) \cdot \frac{\partial^2 y(x,t)}{\partial t^2} + R_{ul} \cdot \frac{\partial y(x,t)}{\partial t} + \frac{\partial^2}{\partial x^2}\left(E_x I(x) \cdot \frac{\partial^2 y(x,t)}{\partial x^2}\right) = F(x,t), \qquad (12)$$

with ρ_r the mass density, $A(x) = w \cdot b(x)$ the variable cross-section, R_{ul} the damping per unit length, E_x the Young's modulus, $I(x) = \frac{w \cdot b(x)^3}{12}$ the moment of inertia, and $F(x, t)$ the force per unit length due to the pressure difference across the reed. The boundary conditions to be satisfied by the equation at the ligature end, which we assume to be clamped are $y = 0$ and $\frac{\partial y}{\partial x} = 0$ and at the free end, they are $\frac{\partial^2 y}{\partial x^2} = 0$ and $\frac{\partial^3 y}{\partial x^3} = 0$. Both Stewart and Strong [44] and Sommerfeldt and Strong [45] used this description of the reed.

In order to take into account the interaction of the reed with the mouthpiece, Stewart and Strong [44] proposed to use varying functions for the reed mass and damping. Sommerfeldt and Strong [45] used a varying function for the damping to take into account the role of the musician's lip as a damper.

The internal viscoelastic losses can be included as proposed by Ricardo da Silva et al. [46]. Completing this model with the damping, Avanzini and van Walstijn [47] as well as Chatziioannou [48] proposed to modify equation (12) as follows:

$$\rho_r A(x)\cdot\left(\frac{\partial^2 y(x,t)}{\partial t^2}+\delta\frac{\partial y(x,t)}{\partial t}\right)+\frac{\partial^2}{\partial x^2}\left[E_x I(x)\cdot\left(1+\eta_r\frac{\partial}{\partial t}\right)\frac{\partial^2 y(x,t)}{\partial x^2}\right]=F(x,t), \quad (13)$$

where the coefficient η_r represents the magnitude of the internal viscoelastic losses and δ accounts for damping of the surrounding fluid.

The interaction of the reed with the lip was modelled by Avanzini and van Walstijn [47] as a linear spring exerting an elastic force in the region of application of the lip and by an increase of the damping δ in this region. The reed-lay interaction was defined as a contact force that acts in the profile of the lay of the mouthpiece. The resulting force relating the pressure difference across the reed to the reed tip displacement is linear for low-level displacements and nonlinear for large displacements. Another result of this numerical experiment was that the reed does not smoothly curl up onto the lay of the mouthpiece, but a discontinuity appears. The authors defined the variable "separation point" as the point of contact between lay and reed that is closest to the tip (the separation point defines which part of the reed is free to oscillate). They showed that the reed does not bend in a smooth way and that the separation point undergoes a discontinuity during reed bending (see Fig. 7). This discontinuity is also observed in the reed equivalent parameters S_r and K_a as shown by van Walstijn et al. [28].

2.2.4 Two-dimensional transverse isotropic distributed models

As the one-dimensional distributed model can not capture any of the torsional modes of the reed that are said to be important for reed quality by some authors [49, 50], a two-dimensional model has been used in other works. In addition, this approach enables to take into account the bending of the reed in the middle of the mouthpiece in the transverse direction while the sides of the reed remain in contact with the mouthpiece rails.

Some models take into account geometry of the reed vamp, i.e. the fact that the reed is thinner at its borders than in its heart. These models assume that the reed material is isotropic transverse and needs five elastic parameters.

Casadonte [13] was the first to perform a numerical modal analysis (ANSYS software) of a reed using a grid of 84 by 33 (2772) points measured on a real reed. He obtained the first twenty modes of a clamped clarinet reed without lip and without mouthpiece. Results show that the first modes are pseudo-torsional modes whereas bending modes are expected. According to Casadonte, this effect could be caused by the asymmetry of the reed.

Ducasse [37] performed a modal finite element simulation of the synthetic reed (Fibracell) of a bass clarinet with free vibrating length of 47 mm using ANSYS, the geometry being defined from measurements. The results show that modes appear as follow: first flexural, first torsional, flexural + torsional modes (Fig. 8).

Facchinetti et al. [49] performed a finite element simulation assuming a linear Love-Kirchhoff plate elements in the CAST3M finite-element code. They used a geometry interpolated from 200 points measured at the reed surface and assumed the reed to be symmetrical with regard to its longitudinal axis. They used five parameters (density, longitudinal and transverse Young's moduli, transverse to longitudinal shear modulus, longitudinal-transverse Poisson's ratio). The modes are labelled $LnTm$ where L stands for longitudinal and n is the number of intersections of nodal lines with the edges parallel to the main axis including the one imposed by the boundary condition at the ligature. T stands for transverse and index m is the number of intersections of the nodal lines with the tip edge of the reed. Results obtained after simulation are similar to the modes obtained by Ducasse and appear in an expected order ($L1T0$, $L1T1$, $L2T0$, $L1T2$, $L2T1$) as shown in Figure 9.

Guimezanes [51] used a finite-element thick-plate model (assuming a linear Love-Kirchhoff plate model) in the CAST3M finite-element code. The reed geometry was interpolated from measurements carried out on 246 points and led to a mesh of 5988 elements. The length of free vibrating part of the reed was set to 35 mm for comparison with experimental results. Modes obtained by Guimezanes are similar to the modes obtained by Facchinetti et al. [49] and Ducasse [58]. The comparison of numerical simulations and experimental results showed that the Young's modulus used in the numerical model should depend on the longitudinal position in order to fit the two sets of results (measurements, simulations) for three different reeds (Young's moduli values given in Appendices A–C).

In his thesis, Chatziioannou [48] proposed an analytical formulation for the deflection of a anisotropic plate and studied a numerical scheme that ensured stability considering the boundary conditions at the edges of a clamped-free plate. He also took into account the effect of the player's lip and of the external driving force between the free end of the reed and the player's lip. He showed that the main difference with the one-dimensional model is that, because of torsional modes, the reed can enter the mouthpiece around the middle of the reed surface. As the reed interior is free to oscillate inside the mouthpiece even when collision occurs at the edges of the reed, the effect of the lay blocking the motion of the reed at its edges is not transferred as strongly to the tip of the reed. As a consequence, high-frequency oscillations preceding every closing of the reed tip are much smaller than those appearing in the one-dimensional case.

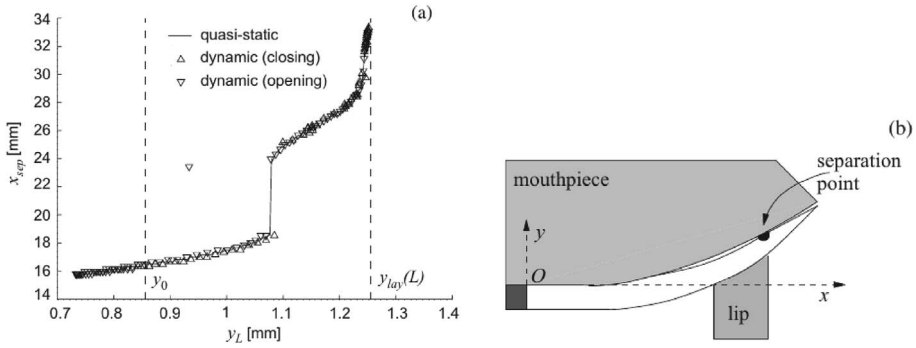

Figure 7. Separation point versus tip displacement [47]; (a) quasi-static simulations (black solid line) and dynamic simulations (y_L is defined as the displacement of the reed tip and x_{sep} as the point of contact between the lay and the reed which is closest to the tip), (b) non-smooth reed curling.

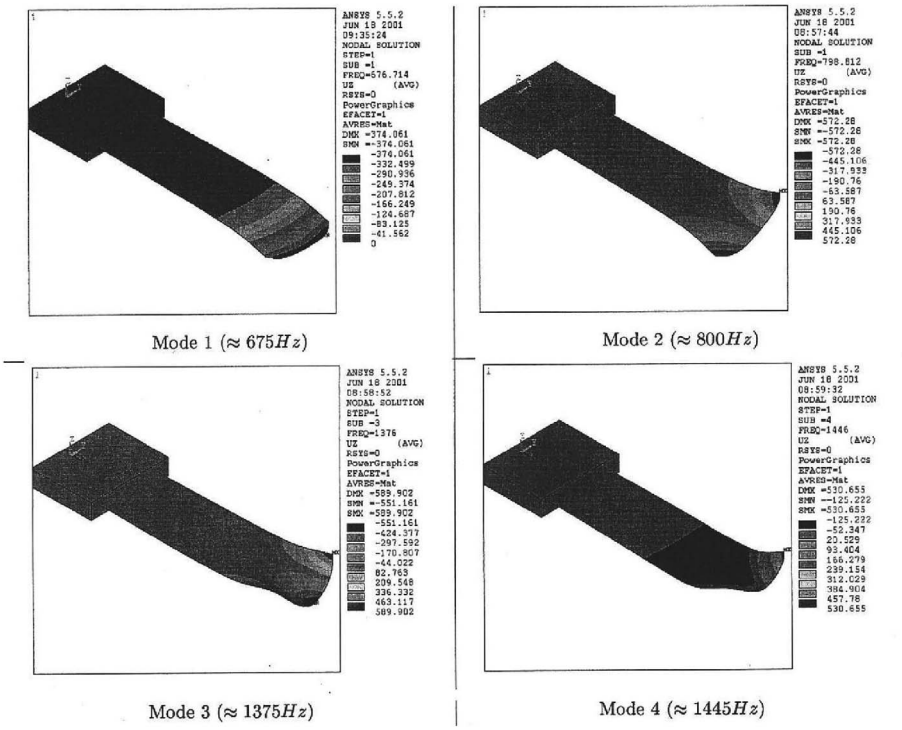

Figure 8. First four computed modes of an isolated reed [37].

This two-dimensional model enabled Chatziioannou [48] to deduce the equivalent lumped model parameters of the reed, the area S_r and the stiffness K_a. The results show that the parameters are nonlinear functions of Δp and that they exhibit a discontinuity (jump) that can vary between "smooth" and "abrupt" (with a jump), depending on both the reed thickness and the lip position. But in this case, because the reed enters the mouthpiece, it is impossible to define a separation point for the entire reed, even though it would be possible to define one at its edges.

Taillard et al. [27] used a FEM simulation of 55 reeds alone (without lip or mouthpiece) in order to estimate the numerical values of elastic coefficients (longitudinal, transverse and radial moduli E_x, E_y, E_z, shear moduli G_{xy}, G_{xz}, G_{yz} and Poisson's ratios ν_x, ν_y). The material was defined as 3D orthotropic and assumed to be homogeneous. The dimensions in the xy plane were consistent with the measurements given by Facchinetti et al. [49]. The generated mesh involved 5927 points. He firstly performed a sensitivity analysis of the elastic coefficients and showed that E_x and G_{xy} play a decisive role, while E_y plays a marginal role and all other parameters have an almost negligible influence on the resonance frequencies. As a consequence, the moduli E_x and G_{xy} are the variables retained in the model. Comparing measured and computed resonance frequencies of 55 clamped reeds with a free vibrating length of 38 mm, Taillard et al. [27] showed that an elastic model cannot predict the 11 eigenfrequencies of the reeds and proposed to use a viscoelastic model in which E_x and G_{xy} are frequency dependent according to a Zener model called also Standard Linear Solid model [52]. This model (Maxwell representation) needs three parameters for each modulus (six

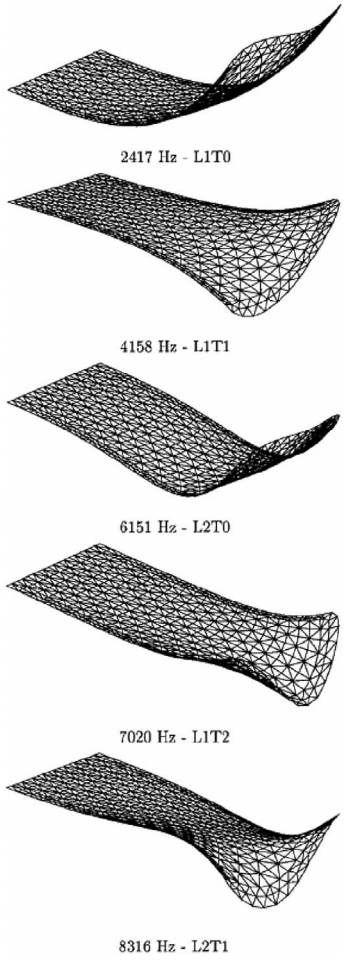

Figure 9. First five computed modes of an isolated reed [49].

parameters per reed). Using a Mean Squared Deviation Method, the optimal parameters were searched assuming that the damping terms in the Zener model are constant, leading to an estimation of two stiffness values per modulus. Results show that the model is valid for "ambient dry" reeds (typically around 55% humidity) in a frequency range which should not exceed one decade.

2.3 Discussion

This section presents the different physical models that can describe the reed behavior. The simplest one considers the reed as a spring. In many papers, the reed is modeled as a Single Degree Of Freedom (SDOF) system in order to take mass and damping into account. To be more realistic, the bending of the reed on the mouthpiece or the contact force between the reed and the mouthpiece can be added, considering a nonlinear stiffness or a nonlinear contact force. More complex models assume the reed as a non-uniform clamped beam or plate.

The process of self-sustained oscillations can be explained by assuming that the reed is a pure stiffness and that the volume velocity entering the reed channel vanishes when the reed closes the mouthpiece. This can be done by solving a two-equations system that describe the resonator and the exciter (reed movement + flow entering the reed channel). In this case, the two important parameters are the reed opening at rest h_0 and the reed equivalent stiffness K_a. These two parameters define the closing pressure $P_M = K_a h_0$ and the threshold pressure $\frac{K_a h_0}{3}$ in the case of a cylindrical resonator without losses. Moreover, according to Dalmont and Frappé [59] and Fritz et al. [60], the musician must blow harder in the case of higher losses of the resonator. Also, Fritz et al. [60] showed that, considering a constant closing pressure P_M, the threshold pressure diminishes when the opening h_0 is decreased.

Considering the reed dynamics (damping, mass) enables to obtain more realistic simulations of the self-sustained oscillations and to understand the effect of these parameters on the pressure signal. Under this assumption, the reed is characterized by four parameters: h_0, K_a, R_a, M_a or h_0, K_a, ω_r and Q_r as in [60]. It can be also characterized by five parameters as proposed in [29] adding $S_d = S_r$ defined in Section 2.2.1. These parameters, coupled with the relative mouth pressure $\gamma = \frac{P_m}{P_M}$ and the embouchure parameter ζ (defined by Fritz et al. [60] and proportional to $\sqrt{\frac{h_0}{K_a}}$) have an influence on the threshold pressure and the frequency of oscillations at the threshold. The study of this influence is a complex topic due to the fact that self-sustained oscillations are produced thanks to a nonlinear dynamic system. If the reed resonance angular frequency ω_r is much greater than the first resonance frequency of the resonator ω_1, approximating the reed as a simple spring is rather good, and the threshold pressure is independent of the reed damping factor. For smaller values of $\frac{\omega_r}{\omega_1}$, then $\frac{\omega_r}{\omega_1}$ and q_r have a impact on the playing parameters (threshold pressure, frequency at the threshold).

According to a study by Karkar et al. [29], the threshold pressure rises with the damping coefficient q_r when taking into account a realistic resonator with frequency-dependent losses. Also, register selection is greatly influenced by the reed damping q_r, which the player controls with his lower lip and higher registers can be played only for low values of q_r, typically lower than 0.5. However, it appears that q_r has a very small effect on the playing frequency.

In a recent work, Petersen et al. [61] developed a simulation tool for simplified clarinets. They showed that the reed resonance angular frequency ω_r has an impact on the threshold pressure, indicating that the "ease of playing" may be related to the reed resonance.

The reed effective area S_d has an influence on intonation and on regime selection [29]. Small values of S_d enable the selection of higher registers with a low frequency deviation, whereas higher values of S_d lead to the selection of the first register with a higher frequency deviation, typically -4% (-68 cents).

The control parameter ζ, which represents the effect of the player's embouchure, in particular the control of the opening h_0, has an influence on the regime selection and on the playing frequency. Results given by Karkar et al. [29] show that for low values of ζ, regime 1 is selected, while for higher values ($\zeta > 0.2$), regime 4 is chosen. ζ has also a noticeable influence on the frequency of the oscillations at threshold. The frequency deviation of the first regime is less

than -0.3% (-5 cents) for $\zeta < 0.2$, whereas the fourth regime frequency deviation is -2.7% (-46 cents) for $\zeta = 0.8$. Finally, for very low values of ζ (when the reed is almost closed), the threshold pressure quickly increases.

Considering the reed as a nonlinear stiffness or considering the contact force due to the interaction between the reed and mouthpiece enables a better explanation of the curling of the reed on the mouthpiece. In this case, the inertial effects appearing when the reed is pressed against the lip and beating effects occurring when the reed closes show clear oscillations on the reed position signal [25] (see Fig. 10).

Finally, considering the reed as a clamped beam explains the interaction between the reed and the mouthpiece. This shows the existence of a separation point evolving with reed displacement (see Fig. 7). Assuming that the reed can be viewed as a 2D system enables us to predict the eigenmodes of the structure and also better explain the interaction between the reed and the mouthpiece. Indeed, using this assumption shows that the separation point is not so clearly defined and that the reed is free to bend inside the mouthpiece while being in contact with the rails, which minimizes the effect of reed beating.

These models provide information about the relationships between the reed equivalent parameters and the playing parameters, such as the threshold pressure and the playing frequency. They can also give information about the internal structure of the reed material. However, the cane material parameters and the equivalent parameters of the reed need to be estimated from measurements in order to feed the models. Moreover, these parameters can have a significant effect on the musician's perception, and this perception needs to be understood. The following section presents the various studies that were carried out to define robust perceptive descriptors that relate to musicians' feedback. Section 4 presents the different experimental approaches developed in order to estimate the values of reed parameters.

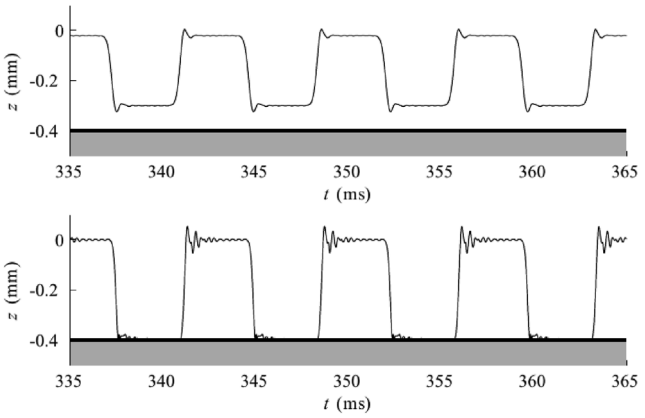

Figure 10. Simulation of the self-sustained oscillations of a clarinet assuming the reed is a SDOF system and considering a force term due to the collision between the reed and mouthpiece lay [25]. Top: steady-state oscillation of the reed position without beating against the lay (illustrated as a grey region at $y = -0.4$ mm). Bottom: reed position under a higher pressure illustrating beating effects.

3 Perceptual assessments of reeds

Reeds are classified by their manufacturers according to their strength and cut. However, large perceptual differences are reported between assumed identical reeds (same manufacturer, strength and cut). According to Petiot et al. [15], who summarized a survey carried out by Muñoz Arancón over 375 musicians [14], clarinet (B♭ and bass) and saxophone (alto, tenor, baritone) players report that in a box of reeds, roughly 30% are of good quality, 40% are of medium quality, and 30% are of bad quality. However, one should note that the reed quality does not only relate to sound perception, but also to the vibroacoustic feedback [62] experienced by the musician during the sound production process described in Section 2. Therefore, the reed quality is often described as "global" [13], "musical" [50] or "overall" [63] as sound quality would only partially reflect the perception by the musician.

Among the numerous studies devoted to the perception of musical instruments [64], a few of them aimed at characterizing the reed quality from the musician's point of view. These studies were conducted over the past 3 decades but their results can hardly be compared because of methodological discrepancies. Namely, the experimental conditions in which the perceptual assessments are carried out largely vary from one study to another. The main differences that can be observed are:

- The number of musicians involved in the test. It can vary from 32 [65] to only 1 [66, 67] that can even be one of the experimenters [55, 68].
- The material under test. It can differ because of the instrument (B♭ clarinet or tenor/alto saxophone) and the reeds (amount and models).
- The assessment method. The reeds can be assessed on the basis of a single quality feature (denoted global/overall/musical) and/or on the basis of more specific criteria (alternatively denoted as quality factors [65], descriptors [13], parameters [68] or abilities [69]).

These main, but not exhaustive, differences between perceptual studies are listed in Table 1, with respect to the terminology used by the authors. The two following subsections are devoted to the description of the assessment methods (quality and criteria) used in these various studies.

3.1 Quality assessment

The reed quality can be determined by assessing a unique perceptual feature on a dedicated rating scale. Casadonte [13] used for this purpose a 7-point "overall quality" scale ranging from "bad" to "good". The "global quality" can also be assessed on a continuous scale, eventually labelled, but this method has been reported to result in large inter-individual differences [14, 15].

As an alternative to scale rating, reeds may rather be categorized with respect to their perceived quality. As an

Table 1. Chronological list of the studies about single reed perception. The subjects and assessment methods are reported following the terminology used by the respective authors.

Year	Material	Subjects	Assessment
1995 [13]	Clarinet (100 reeds)	10 clarinet students (professional or preprofessional)	Overall quality 5 descriptors
1998 [69]	Clarinet (60 reeds)	2 experienced clarinettists (including 2nd author)	6 abilities (averaged as overall quality category)
1999 [65]	Clarinet (10 reeds)	32 clarinet players (professional)	5 quality factors
2003 [50]	Clarinet (24 reeds)	2 clarinet players (professional soloists)	Musical quality (4 categories)
2007 [68]	Alto/tenor saxophone (25 reeds)	1 experienced musician (3rd author)	6 parameters (averaged as overall quality score)
2014 [70]	Clarinet (9 reeds)	2 clarinet players (professional and author)	Musical quality (good/mediocre)
2016 [66]	Clarinet (200 reeds)	1 expert musician (professional reed tester)	3 descriptors
2016 [71]	Clarinet (27 reeds)	2 professional clarinetist	1 parameter (3 categories)
2017 [15]	Tenor saxophone (20 reeds)	10 saxophone students (skilled musicians)	Global quality 2 descriptors
2017 [14]	Tenor saxophone (20 reeds)	7 musicians (amateurs and professionals)	Global quality 2 descriptors
2018 [55]	Clarinet (40 reeds)	1 professional clarinetist (author)	2 descriptors 2 abilities
2020 [67]	Alto saxophone (8 reeds)	1 jazz musician (professional)	1 parameter (ranking)
2022 [72]	Tenor saxophone (12 reeds)	1 professional saxophonist	Dissimilarity 4 criteria
2023 [63]	Clarinet (13 reeds)	2 experienced musicians (including 1st author)	Overall quality (good/bad)

example, Pinard et al. [50] classified the reeds as "very poor", "poor", "good" and "very good" on the basis of the "musical quality". A binary categorization of the reeds can also be proposed to discriminate between good and mediocre reeds with respect to "the musical quality" [70] or between good and bad reeds with respect to "the overall quality" [63].

3.2 Criteria assessment

As large discrepancies can be observed among global quality assessments [14, 15], some authors decided to focus on more specific criteria. Such perceptual assessment can be carried out in addition to quality assessment in order to study the correlation between the criteria and the overall quality, as did Casadonte for the following descriptors: "timbre", "strength", "noise", "stability" and "acoustic strength" (rated each on a 7-point scale). Obataya and Norimoto [65] carried out subjective reed assessments on the basis of five "quality factors": "sonority", "richness", "softness", "ease of vibration", and "response" (translated from Japanese) as an alternative to a unique quality feature. Gazengel et al. [66] assessed three descriptors: "ease of playing", "brightness" and "roundness". Two of these descriptors, "ease of playing" and "brightness", were kept by Petiot et al. [15] and Muñoz Arancón [14] in subsequent studies. One should, however, note that "ease of playing" is alternatively denoted as "softness" [15] and "brightness" as "timbre" [14]. Gangl et al. [71] also categorized the reeds according to their "playing ease". Taillard [55] assessed the reeds himself according to two descriptors ("subjective strength" and "intonation") and to their abilities to play the first lines of particular musical pieces (a Poulenc sonata and a Schubert lied). Parameter assessment can also be used to obtain a reed ranking, as did Kemp and Scavone [67] in order to rank the reeds with respect to the "perceived stiffness".

Such abilities and parameters can also be used to derive an overall quality score. Kolesik et al. [69] carried out subjective assessments by two "experienced clarinettists" according to the abilities of the reed to produce:

- "a clear tone over the range of the instrument",
- "clear and rapid articulations over the range of the instrument",
- "smooth slurs between high and low notes",

and to play:

- "the note F_6 (clarinet pitch) with the conventional fingering in tune",
- "the note A_9 easily and in tune",
- "without great effort upward to C_7".

Each reed was subsequently categorized as "good", "fair" or "poor" overall quality on the basis of its average performance along these abilities. Similarly, Mukhopadhyay et al. [68] defined the reed "overall quality score" as the average of the ratings on the following parameters: "ease of attack", "ease of sustenance", "tone quality in the low, middle, and high ranges of the instrument", and "score for volume".

In all, one can observe a large variety in the criteria studied from one study to another. On one hand, two different descriptors assessed in a single study may prove to be highly correlated (e.g., "ease of playing" and "brightness" [66]). On the other hand, a descriptor designed to describe the same perceptual feature may be designated by different terms across studies (e.g., "ease of playing"/"softness" [15, 66] or "brightness"/"timbre" [14, 66]), despite being conducted by the same coauthors. As a result, the correlation between "ease of playing" and "brightness" highlighted by Gazengel et al. [66] was subsequently reaffirmed by Petiot et al. [15] who reported "softness" to be correlated with "brightness", as can be seen in Figure 11.

In order to tackle the semantic issue related to criteria definition, Koehl et al. [72] tried to identify the perceptual

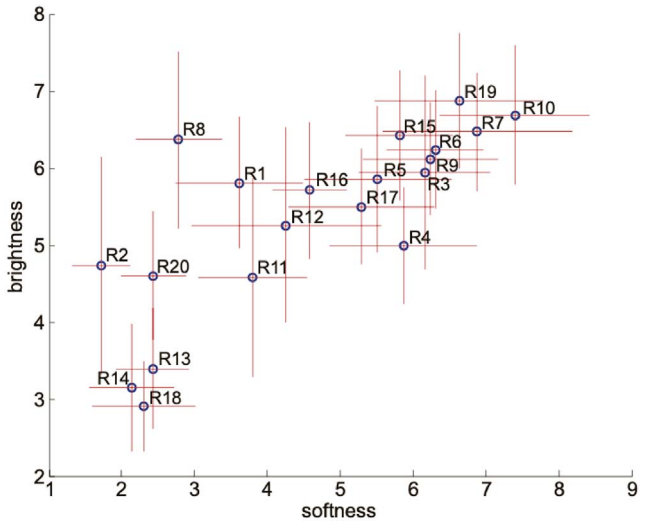

Figure 11. Relationship between "softness" and "brightness" assessments (average within 95% confidence interval) for 20 reeds [15].

dimensions that are used to differentiate between reeds. By using a similar approach as the one used to identify musical timbre dimensions thanks to multidimensional scaling [73], dissimilarity judgments were obtained for 12 reeds in paired comparisons. The timbre of wind instruments [74], saxophone [75] and clarinet [76] has already been studied this way, but from the listener's point of view. However, the difficulty of performing dissimilarity judgments (66 pairs) for a professional saxophonist in a playing situation led to even less reliability than when assessing the four criteria defined by the musician himself ("strength", "color", "emission" and "reactivity").

3.3 Summary about perceptual reed assessment

All the perceptual studies cited above are chronologically ordered in Table 1. To sum up, one can observe large methodological differences between these studies that do not enable so far to draw general conclusions about perceptual reed assessment. Therefore, the establishment of relationships between perceptual assessments and physical properties of the reeds is not straightforward.

In addition, large variations in the experimental conditions may also be observed within one given study. As an example, all the subjects involved in a study are not necessarily asked to assess the same reed subset [13]. The perceptual assessments may also be carried out by using different instruments [15] or mouthpieces [50] when the subjects were allowed to use their owns. All these discrepancies do not facilitate the prediction of perceptual assessments by physical characteristics.

Nevertheless, the physical measurements that were carried out alongside the perceptual assessments (and that are described in Sect. 4) still enabled to highlight physical correlates of global quality, ease of playing, intonation (or playing frequency [3]), and timbre (mostly brightness).

4 Physical measurements on reeds

The studies presented in Section 3 are dedicated to perceptual tests, but they also include physical measurements in order to establish relationships with perceptual observations and to possibly predict the reed qualities prior to perceptual assessment by musicians. In addition to these studies, several other ones were solely devoted to the physical characterization of the reeds. An exhaustive list of the measurement methods is structured in Figure 12, where the studies including also perceptual assessments are indicated in bold. The present section describes the measurement methods presented in Figure 12. The link between perceptual assessments presented in Section 3 and physical measurements presented here is presented in Section 5.

The physical measurements can be gathered into two main categories, namely destructive and non-destructive methods.

Destructive methods were designed to study the material parameters. Once the reed is cross-cut, the inner structure of *Arundo donax* can be observed thanks to optical measurements with microscopes. Mechanical measurements, in either static or dynamic conditions, can also be carried out to measure material properties such as stiffness or Young's modulus. As the reeds are always destroyed prior to characterization, these methods are generally applied to small reed samples and cannot be used for industrial purposes.

Non-destructive methods were then designed to avoid this main drawback; they are of two types. On the one hand, the sole reed can be studied to measure several physical parameters. Among others, its external geometry, its global or local stiffness, and its vibration modes can be measured. On the other hand, reed behavior can be observed in playing situations with either an artificial or a real musician. Reed parameters (equivalent stiffness for example), playing parameters such as frequency, spectral centroid, threshold pressure, and sound pressure level are estimated using signal analysis. The link between these parameters (perceptual descriptors and reed physical parameters) enable to better understand the role of the reed.

The typical numerical values of the parameters presented in the section are presented in Appendices A–C.

4.1 Destructive methods

The purpose of destructive studies is to get insight into the reed material *Arundo donax* by measuring its physical properties. The design of a destructive study begins with the collection of reed samples extracted from the heel (i.e. the reed's thickest part). The reed sample can be directly observed from a microscopic point of view to gather information about the biological structure. The structure of the different type of cells and vascular bundles is revealed. Reed samples can also be submitted to mechanical tests to measure the mechanical properties of *Arundo donax*, in either static or dynamic conditions. The material stiffness is measured in static conditions, whereas the Young's modulus can be measured in both static and dynamic conditions.

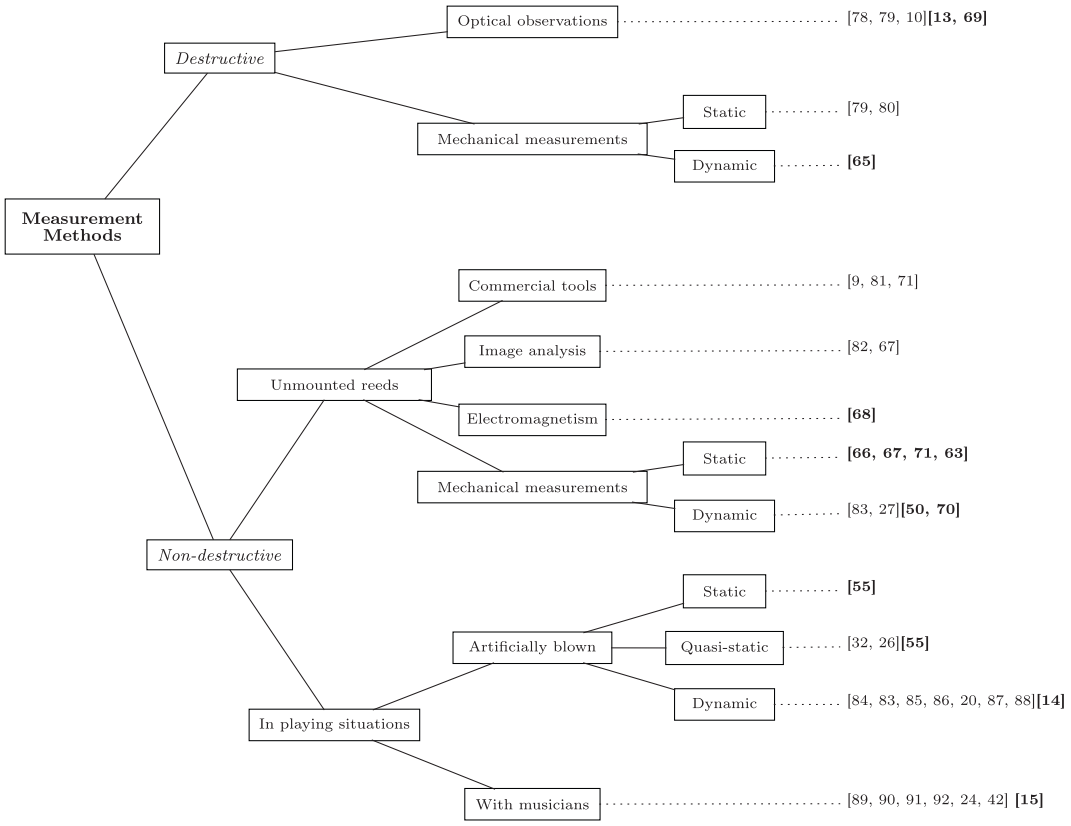

Figure 12. Overview of the different methods to study single reeds. A perceptual study was carried out for references in bold.

Optical observations

Reserchers from ITEMM [77] observed the reed cross-sections. A thin slice of a clarinet reed heel is observed thanks to tomography. The cross-section is made of two main parts: firstly the outer part and secondly the inner part depicted in Figure 13.

The epidermis and the fiber band are on the outer part of the cane. These layers are completely removed from the vibrating part of the reeds. The inner part of the cane is called cortex. It contains a matrix called parenchyma made of compliant cells accounting for 43%–57% of the whole cortex [10, 78]. Parenchyma is inlaid of vascular bundles as presented in Figure 13. Inside, the plant blood vessels (namely phloems and xylems) are surrounded by a rigid fiber ring. The fiber ring is oriented along the length of the cane, forming a long tube. Thanks to scanning electron microscopy, Casadonte [13] observed that the number of vascular bundles increases from the inside to the outside of the cane radius. Kolesik et al. [69], Kawasaki et al. [80] and Veselack [10] reached the same conclusions.

Firstly, reeds differ in the quality of their fiber rings. Some have wide and continuous fiber rings as shown in Figure 13 whereas some have just a few fiber ring cells. Secondly, reeds have different proportions of vascular bundle fibers and parenchyma cells. Veselack [10] and Kolesik et al. [69] reported that the growing environment of cane impacts the cells structure. As an example, fast-growing and immature canes present larger cells and thinner cell walls. Canes grown in a plantation have a bigger proportion of vascular bundles with a continuous fiber ring than wild canes. Moreover, canes from crops have a higher proportion of fiber and a lower one of xylem [69].

Mechanical measurements

Fibers constituting the fiber ring shown in Figure 13 are responsible for the cane rigidity. Indeed, the fiber ring cells have a higher Young's modulus than the parenchyma cells. Consequently, the mechanical properties of the reed depend on the quantity, quality and distribution of fibers within the material. The mechanical properties of the materials can be assessed under both static and dynamic conditions.

In static condition, the object is measured thanks to a force that is constant in time. Generally speaking about reed mechanics, this type of measurement is used to obtain mechanical parameters such as stiffness and Young's modulus. A nanoindentation system was used by Kawasaki et al. [79] to measure the Young's modulus of clarinet reeds heel samples. In the longitudinal direction (from the heel to the tip, in the direction of the fibers), this parameter reaches 7 GPa. Ukshini and Dirckx [80] were also interested in observing the static parameters of reeds. By applying a punctual force to tenor saxophone reed heel samples, he measured longitudinal (E_x) and transversal (E_y) Young's moduli. The resulting E_x (5 GPa) is 10 times greater than E_y (0.5 GPa), making *Arundo donax* a highly anisotropic material. This result is of the same order of magnitude as

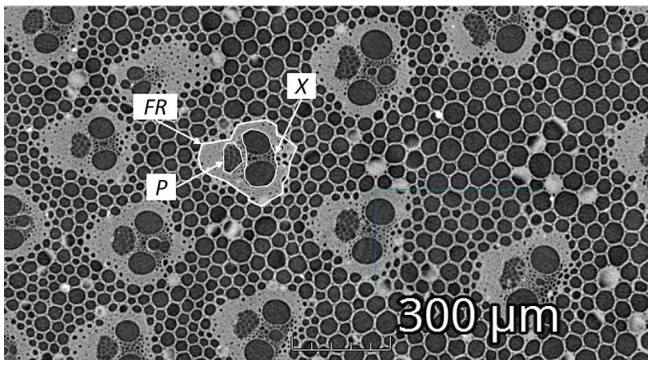

Figure 13. Tomographic reconstruction of the inner part of *Arundo-Donax*. This picture has been provided by ITEMM [77] (FR = fiber ring, P = phloem, X = xylem).

Kawasaki et al. [79]. A comparison between a wet and a dry specimen showed that both E_x and E_y are lower for the wet reed (respectively 3.1 GPa and 0.1 GPa), with an increasing difference in the transversal direction [80]. As a consequence a wet reed is more flexible than a dry one.

The chemical composition of the plant can explain this observation. In fact, parenchyma cells are filled with cellulose and contains glucose, fructose and sucrose which are water-soluble extractives. As a consequence, in contact with water or musician's saliva, the substances are extracted from the cells [78]. This may cause a shrinkage of the cells and changes in the mechanical behavior of the reed. Long term effects can cause excessive deterioration of the reed. Obataya et al. [65] tried to understand this phenomenon thanks to a dynamic measurement method.

They studied the role of the extractives on the reed properties (dynamic Young's modulus, internal friction) using dynamic measurements with various levels of relative humidity and different excitation frequencies. Especially, a free-free beam flexural method was used. In this way, vibrational modes were studied via the estimation of the eigenmodes and modal parameters. Obataya et al. [65] compared the dynamic Young's modulus (E') of chemically modified samples of reeds. Some were freed from the water-soluble extractives and among these, some were impregnated with glucose. Their behavior was compared to untreated reeds, as shown in Figure 14. E' of untreated and glucose-impregnated reeds have the same evolution even if it is constantly smaller by 0.5 GPa for the glucose-impregnated reed. E' increases with frequency (Fig. 14a) and decreases with the level of ambient relative humidity (RH) measured in a closed box (Fig. 14b). The effect of RH on the E' of water-extracted reeds is negligible.

It should be noticed that the extracted reeds and the glucose-impregnated reeds have respectively a smaller and a higher density than the untreated reeds.

4.2 Non-destructive methods

In Section 4.1, several studies applying destructive methods to reeds were presented. Both biological and mechanical material parameters can be estimated this way. The information gathered provides a better understanding of the material structure but remains insufficient to fully characterize reeds. Specifically, several conclusions drawn from these studies cannot be extended to the whole reed as the cross-section is not constant. Moreover, the destruction of the reeds rules out the possibility of using these methods for industrial purposes.

Instead, non-destructive methods can be used, firstly on the reed itself without mouthpiece or resonator. The external geometry of the reed can be verified using manual measurements of the reed cut or by image analysis. Images can also reveal the internal structure of the reed and the geometrical arrangement of fibers from the tip to the heel. Electromagnetic and mechanical setups can be used to measure structural parameters. In static conditions, stiffness and compliance (i.e. the inverse of stiffness) of the reed tip can be estimated. In dynamic conditions, vibrational modes of the reeds can be characterized by their shape and eigenfrequency, as well as material parameters such as shear and Young's moduli.

Secondly, the reed can be studied in a playing situation, with an artificial player or a real musician. This time, the reed is an integral part of the exciter coupled to the resonator. Various signals can be recorded using sensors and microphones incorporated into the instrument. With these acquisitions, it is possible to observe the movement of the reed in interaction with its environment, estimate the reed parameters, and estimate parameters related to the signal produced by the instrument.

4.2.1 Unmounted reeds

The simplest way to measure reed parameters is to consider the reed alone to avoid the effect of mouthpiece and ligature. Even musicians can proceed to easy measurements since commercial tools have been designed. They enable to control some reed parameters and eventually adjust them when needed. For this purpose, Groom [9] developed a manual single reed micrometer accurate to one-thousandth of an inch (25.4 µm). It enables the musicians to measure the reed thickness over a 35-points mapping and control the regularity of the cut (i.e. shape, also known as profile). According to her, this device is intended to help the musician to enhance the reed quality. He may recover the reed lateral symmetry by adjusting the thickest part of the reed. Hanai [81] designed another test rig using the same self-made measurement principle on several points. Instead of estimating the reed thickness, the rigidity of the reed is measured. More information about this type of measurement is provided in the following paragraph *Mechanical measurements*. Gangl et al. [71] were also interested in manual measurements and used a third type of commercial tool aiming at estimating the hardness of the material. They only concluded that this method cannot be used to compare reeds of different materials or strength.

To take this a step further, the researchers have developed other measurement benches designed for research and not for commercial use.

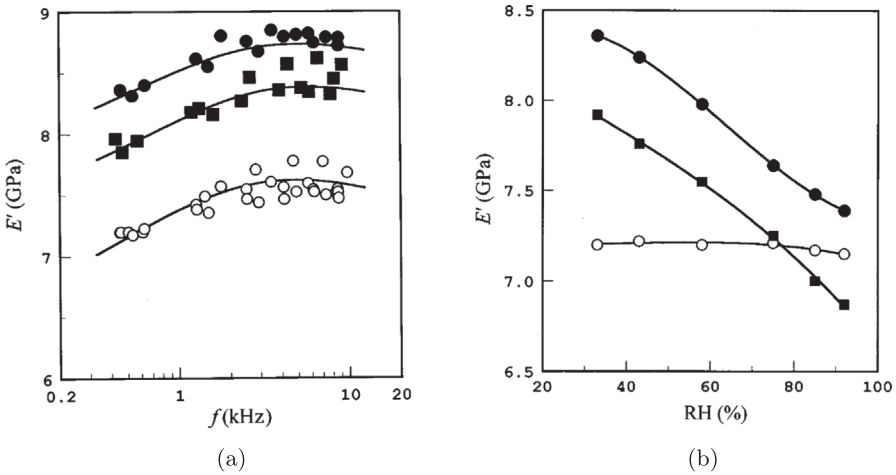

Figure 14. Effects of frequency and relative humidity on the dynamic Young's modulus of untreated (black dot), water-extracted (white dot) and glucose-impregnated (black square) reed from Obataya et al. [64]. (a) Evolution of E' at 33% relative humidity plotted against frequency. (b) Effect of relative humidity (RH) on E' at the first vibrational mode.

Image analysis

The profile geometry of the reed can be analyzed thanks to image analysis. Cazalans et al. [82] experimented X-ray microtomography. This technique results in pictures of multiple longitudinal or transversal slices of the measured reed. In addition to being very accurate, this technique provides information on the internal structure of the reed. In particular, the amount of cane fiber and its distribution across the width of the tip can be examined. Thanks to microscopy, Kemp et al. [67, 93] observed the fiber distribution along the entire length of the reed. The conclusion of this work was that most fibers are continuous from the heel to the tip of the reed. Figure 15 illustrates this observation.

Electromagnetism

The inner structure of the reed can be studied by employing planar electromagnetic sensors as suggested by Mukhopadyay et al. [68]. They indirectly measured material parameters such as dielectric permittivity ε measured in, magnetic permeability μ measured in and electric conductivity σ measured in by using a specially designed sensor. It does not appear to be a direct method for assessing the contribution of the three parameters to the transfer function. Nevertheless, the authors believe that dielectric permittivity is the most important characteristic responsible for the differences in reeds behavior as it resulted in a frequency shift in the phase response of the sensor.

The method provided promising results in the high frequency domain but required expertise in sensor implementation and expensive state-of-the-art technology. As a result, no one has attempted to take this approach any further.

Mechanical measurements

As for destructive methods, the mechanical properties of the reed itself can be studied under static and dynamic conditions.

Measurements under static conditions are an interesting option. In fact, this method is a major part of the reed manufacturing process. The reed strength, which is usually indicated on the reed by a number between 1 and 5, is typically measured this way [8]. It can be obtained by using an automated measuring bench that imposes a linear displacement across the entire width of the reed tip. The force induced by this displacement directly provides the reed strength.

Gazengel et al. [66] measured saxophone reeds in the same way. The heel of the reed was fixed and the vamp remained free. A spring with a known stiffness bends the reed tip. In this way, both the reed tip displacement and the force induced by the spring were known. From these two variables, the authors deduced reeds compliance (inverse of stiffness). Alongside the static compliance, they measured the dynamic compliance of each reed. These two quantities were found to be highly correlated, with a correlation coefficient $R = 0.99$. In addition to global reed compliance, it may be interesting to measure local reed compliance. In this way, measurements can be used to further differentiate between reeds. Reeds may have identical overall compliance but differ locally in width or length. This idea was followed by Hanai [81] to design his own commercial test rig (previously presented in Sect. 4.2.1). Gangl et al. [71] investigated local compliance using the same technique as Gazengel et al. [66]. The compliance was measured in three points aligned on the reed center at 0 mm, 8 mm, and 16 mm from the tip and compared for 9 cane and 18 synthetic reeds of different strengths. Similar stiffness values were obtained for reeds of the same strength but made of different materials.

Kemp et al. [67] were also interested in local stiffness measurements on clarinet reeds. Reeds were studied through the measurements at 3 points distributed over the width at 1 mm and 4 mm from the tip. The first conclusion of this work is that the local stiffness of the tip is correlated with the local amount of vascular bundles.

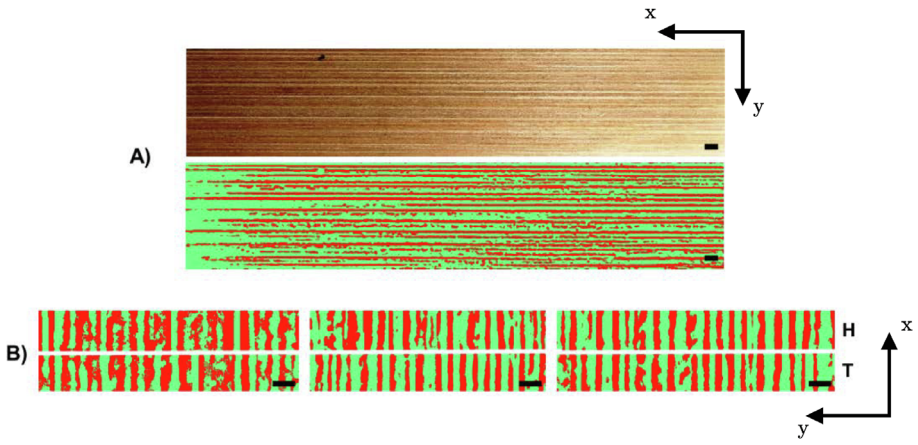

Figure 15. A: optical and corresponding segmented images of the underside of an alto saxophone reed ($z = 0$ according to Fig. A1), with identified solid fibers shown as shaded/colored regions. B: reed tip (T) and heel (H) subsections of segmented images for three reeds. Black scale bars are 1. Adapted from Kemp [92].

Secondly, investigations about the evolution of reeds over time revealed that the more the reed is played, the more the reed tip stiffness decreases. After 300 min of playing, the reed stiffness has decreased by almost 45%. Finally, Gaillard et al. [63] also designed a test rig to measure local stiffness. The main objective of this experimentation was to measure the stiffness symmetry of the reed tip. For this purpose, stiffness measurements were carried out at 11 points distributed over the width at 3 mm and 10 mm from the tip. The stiffness profile obtained was then approximated by a parabola where one of the coefficients indicates the maximum stiffness of the reed tip. Its values were of the same order of magnitude as the measurements by Kemp et al. [67]. Another coefficient was found to indicate the lateral position of the maximum which quantifies the asymmetry of the reed tip. An example of measurements can be seen in Figure 16.

To better understand the physical behavior of a reed in a playing situation, it is important to consider it under dynamic conditions. This can be obtained thanks to a forced excitation that is usually applied by a loudspeaker located in the mouthpiece or in a cavity close to the reed [66]. This method enables to reveal the shapes and eigenfrequencies of vibrational modes. To carry out such measurements, optical methods as holography were used by Pinard et al. [50], Picart et al. [83], Stetson [70] and Taillard et al. [27]. This non-invasive technique consists in projecting a monochromatic light from a LASER on the reed. The phase of the reflected light on the reed is recorded by interferometry and compared to the phase of the reference ray [94]. Three different categories of modes can be identified on simple reed, as some examples can be seen in Figure 17: flexural modes, torsional modes and mixed modes.

According to Pinard et al. [50], the reed quality relies on the presence and symmetry of the first torsional mode. They concluded that the symmetry enabled a uniform air flow and an easier sound emission. In order to verify this assumption under more realistic conditions, they reproduced the same measurement when humidifying each reed beforehand. The conclusions were the same, but the modes appeared at lower eigenfrequencies for humidified reeds. As an example, for the first bending mode, the resonance frequency of a clarinet reed dropped from 2200 Hz to 1800 Hz. Stetson [70] reached the same observation. This is in agreement with the fact that moisture adds mass to the vibrating part and reduces its rigidity. Taillard et al. [27] showed that the eigenfrequencies of these flexural modes depend on the longitudinal Young's modulus (E_x). For the torsional ones, they depend on the shear modulus in the tangential plane (G_{xy}). For the mixed modes, the frequencies depend on both (G_{xy}) and (E_x). Then, they designed a numerical simulation of a viscoelastic model by Finite Element Method (FEM) which confirmed these experimental observations for the first fifteen modes.

All these measurement methods appear to be suitable for studying the reeds themselves. They have proven their efficiency but do not provide information about the reed behavior in real playing condition. Firstly, the boundary conditions were generally not realistic, as the reed was typically not clamped on a mouthpiece. As a consequence, the reed could not bend on the mouthpiece rails as it should in a playing situation. Secondly, even if the reed was attached to a mouthpiece and able to vibrate, as it was the case for dynamic holographic measurements, the excitation level was far below what can produce a real musician. The level of excitation is around 100 dB SPL for a loudspeaker whereas it can reach 150 dB SPL in a real situation. Thus, to go further in reed understanding, measurements in artificial or real playing conditions were designed.

4.2.2 Reeds in playing conditions

Artificial conditions

The first approach consists of using an artificial player. This makes it possible to observe the reed behavior in repeatable playing conditions. For this purpose, the reed is attached to an instrumented mouthpiece (clarinet or saxophone) with a ligature. The mouthpiece is equipped with

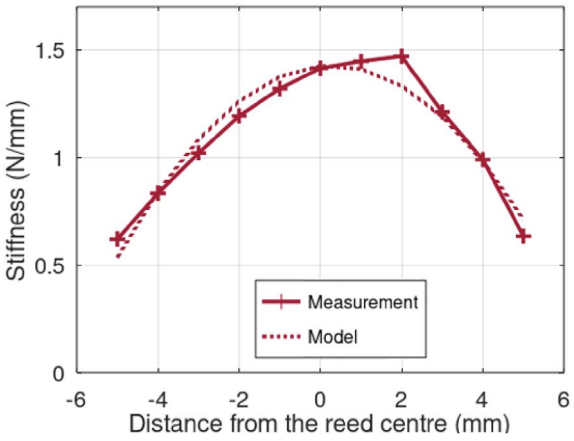

Figure 16. Stiffness profile at 3 mm from the tip of a clarinet reed and its approximation by a parabola.

various sensors measuring pressure, displacement, or force. An artificial lip and a resonator are added to the device.

Two types of artificial musicians can be designed, as shown in Figure 18. An artificial musician of the first type applies an overpressure at the entrance of the mouthpiece (Fig. 18a). The mouthpiece and sensors are located in a hermetic enclosure modelling the mouth cavity. By increasing the air pressure in the box, as the musician would do in his mouth, the reed vibrates. It is also possible to design an artificial musician of the second type by applying an underpressure at the end of the mouthpiece (Fig. 18b). In this case, the mouthpiece is in the open air. In the same way as for the first type, the pressure difference allows the reed to vibrate, which induces self-sustained oscillations. This kind of device is more convenient to study reeds since it does not necessitate to open the box to replace the reed. However, this test rig does not allow the use of a side-hole resonator. As the resonator is a cylindrical tube, only one note can be played.

Using an artificial musician enables to study the reed in different conditions, such as static, quasi-static, and dynamic, which is not possible with a real musician.

In static conditions, the device is partially used as it does not apply any air pressure variation. This type of measurement makes it possible to estimate the channel opening as a function of the lip position alongside the z-axis (see Fig. A1 in Appendix A). Taillard [55] designed such a system. He recorded the distance between the reed tip and the mouthpiece for 40 new reeds at 16 lip positions in the z direction. Each lip position induces a force distributed on the reed along the y-axis but he did not record it. The measurement was repeated after a break-in on these same reeds in 25 positions. Taillard pointed out two consequences of the break-in process. According to him, the reed channel height becomes smaller and the reed tip undergoes a slight deformation.

In quasi-static conditions, both the overpressure system [26] and the underpressure system [32, 56] can be used. Pressure variations are here applied by the system, but in such a way that the reed does not vibrate as in playing conditions. Such measurements are conducted in order to validate models of the nonlinear characteristics of the reed and mouthpiece, as illustrated by the equation (6). It is also possible to estimate reed parameters such as the initial opening of the reed channel h_{00}, the closing pressure P_M or the leakage cross-section [32]. Dalmont et al. [26] designed an overpressure artificial musician that enabled them to increase the pressure in the mouth cavity until the reed completely closed the channel. Then the pressure gradually decreased until the reed channel opened to an equilibrium position. While the pressure changed, the height of the reed channel was measured. This process may be repeated for several lip positions.

Taillard [55] plotted the aeraulic section S as a function of pressure drop Δp for 7 different lip forces on the reed. It appeared that all functions contained a straight line of identical slope. Gazengel et al. confirmed this result [32] that is summarized in Figure 19. The characteristic of the system appears to be nonlinear when the reed bends on the mouthpiece rails. Dalmont et al. [26] also carried out such measurements and concluded that the reed stiffness is approximately the same for an increase or decrease in pressure. In addition to this observation on the reed opening, they obtained the nonlinear characteristic of volume flow as a function of pressure. For both measurements, the theoretical and experimental curves were superimposed, which validate the two-equation model (Eq. (5)) which ignores the reed dynamics.

In order to gain insight about the reed behavior in a situation that is close to a real musician playing, self-sustained oscillations shall be used in order to create realistic vibration levels. Experiments with artificial musicians in dynamic conditions can provide information about the reed vibration parameters as frequency and displacement. Both periodic (i.e. producing a note of the tempered scale) and chaotic (i.e. producing an unpleasant squeak) regimes can be created [86] by adjusting the lip force and the mouth pressure. The next part of this article is devoted to periodic regimes obtained with artificial musicians in dynamic conditions.

McGinnis et al. [84] used an artificial player combined with a stroboscope to measure the vibration frequency of a clarinet reed. They firstly observed that the reed vibration frequency is the same as the expected fundamental frequency of the tone produced. Thompson et al. [20] justified this observation by pointing out that the sound quality is better when the reed vibration frequency is close to the playing frequency, as the production of energy is maximized. As a result, the oscillation of the air column is stabilized by increasing the feedback at the reed frequency. Besides, it has been shown that the reed channel opening surface is proportional to the mouthpiece pressure [87].

McGinnis et al. [84] secondly showed that a complete cycle of reed displacement included complete closure of the channel. Backus et al. [88] completed this statement by reporting that the channel was closed during half of the cycle for loud tones for the clarinet. The closure time decreases as intensity decreases, so that the channel remains open for very soft sounds. Picart et al. [83] confirmed this

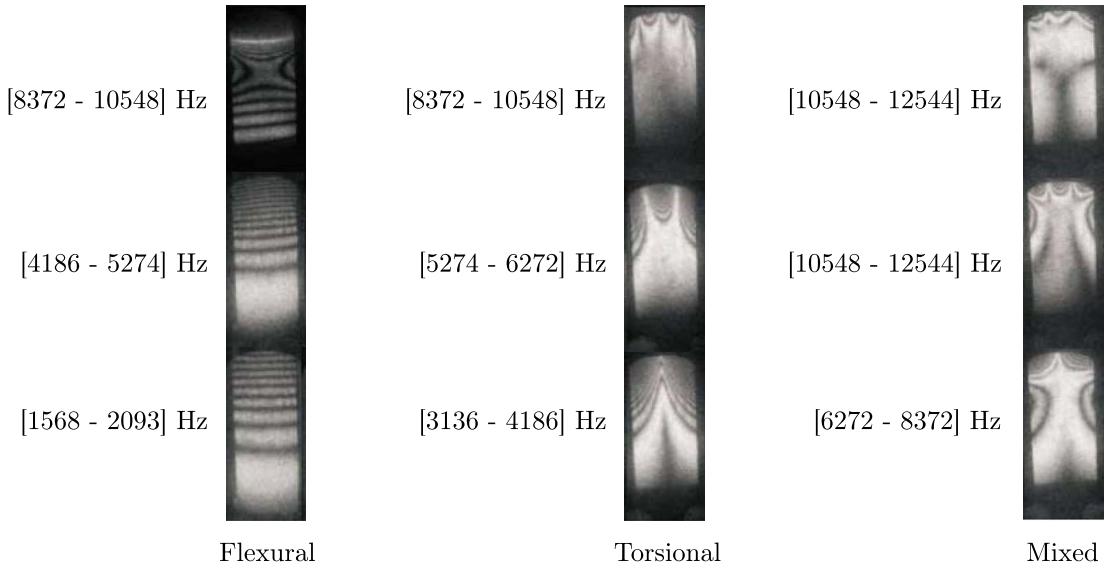

Figure 17. First 3 modes of each type (Flexural, Torsional and Mixed) of a dry clarinet reed with their frequency ranges obtained by Taillard et al. [27]. This figure is adapted from their work.

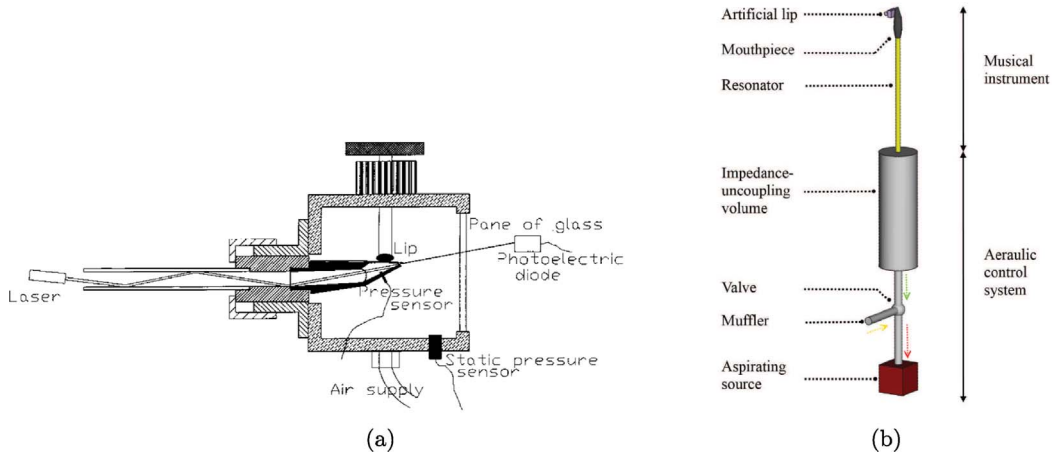

Figure 18. Sketches of two different artificial mouth systems. (a) Artificial mouth designed by Dalmont et al. [26] with overpressure system. (b) Artificial mouth designed by Muñoz Arancón et al. [95] with underpressure system.

finding and went even further by decomposing the reed displacement for very loud sounds in four steps as shown in Figure 20. The channel is open between letters A and E. From E et F, the channel is closing and the reed is wrapping around the mouthpiece until J. It should be noticed that the reed bounces on the mouthpiece at point G. Finally, the reed moves away from the mouthpiece to reach the maximum opening at A.

Picart et al. [83] also confirmed the theory of McGinnis et al. [84] about the shocks between the reed and the mouthpiece when the regime of the beating reed is reached. These shocks are likely to highlight high-rank modes of the reed which contribute to the production of a "metallic" sound. The authors concluded that the local material properties at the tip of the reed play a prominent role in the vibrational behavior of the reed and, by extension in the timbre. This effect on the timbre is caused by the interaction between the reed and the mouthpiece as the high-level vibrations of the reed are constrained by the mouthpiece lay geometry [87]. Ukshini and Dirckx [85] were also interested in this phenomenon which led them to study 3D vibrational pattern of saxophone reeds in relation to different mouthpieces. They used an artificial musician with two high-speed cameras to record the reed movements and a microphone at the bell of the instrument. They concluded that the shape of the mouthpiece and the lip force both change the amplitude of the reed vibration and its harmonic content. In addition, it appeared that the first bending mode of the reed is the most present compared to any other mode.

Artificial musicians do not represent the exact same playing conditions as real ones since the control parameters are only estimates. On the one hand, clarinetists and

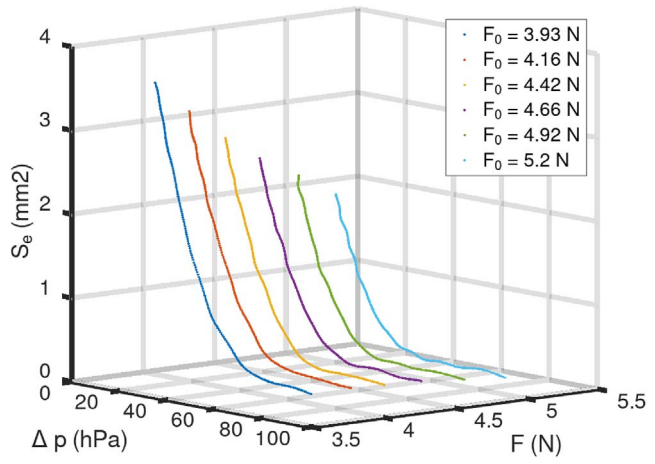

Figure 19. Effective section S_e as a function of pressure Δp for 6 different static lip forces F_0, adapted from Gazengel et al.[32].

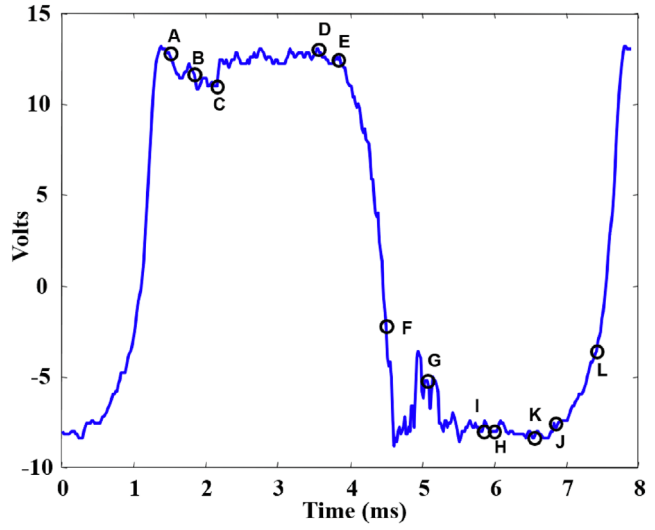

Figure 20. Reed displacement during one period of vibration measured by Picart et al. [82]. The reed channel is open between letters A and E. The channel is then closing until F and opens again from letter J.

saxophonists adjust the geometry of their vocal tract to modulate the timbre of their instrument [96–100]. On the other hand, the role of tongue shape and displacement is crucial in pitch and articulation control [90, 101]. Neither the effect of the vocal tract nor that of the tongue is taken into account when using an artificial musician, except in [43, 102] where the authors use an artificial mouth equipped with an artificial tongue. Only the volume of the hermetic box can be controlled to be similar to that of a musician's mouth [103]. Nevertheless, a significant relative difference has been observed in the reed displacement between artificial and real musicians that can reach up to 30% [95]. To avoid these problems and to better understand the way real musicians play their instruments, real-condition experiments are designed. Therefore, instrumented mouthpiece and recordings of the acoustic pressure at the instrument's bell are used.

Real conditions

Measurements in real conditions may be conducted for three main reasons, detailed below:

- to better understand how musicians play their instrument and use it for educational purposes,
- to estimate reed parameters via signal processing,
- to estimate playing parameters such as playing frequency, sound pressure level, threshold pressure.

Firstly, these measurements are made to better understand how clarinetists and saxophonists play their instrument. By using an instrumented mouthpiece, it is thus possible to obtain pressure values in the musician's mouth and mouthpiece. Fuks et al. [88] conducted such experiments with musicians. Thanks to pressure sensors integrated in clarinet and alto saxophone mouthpieces, they recorded the blowing pressure in the musician's mouth for different pitches and dynamic levels. The pressure typically ranges from 2.0 kPa to 5.9 kPa and from 1.3 kPa to 8.3 kPa, for clarinet and saxophone respectively. Even if these measurements are not directly related to reeds, they may contribute to their study. Indeed, realistic pressure levels could be applied to artificial musicians. Pamiès-Vilà et al. [90] measured the same order of magnitude for the mouth pressure of clarinet players. In addition, their results showed that mouthpiece pressure is higher, reaching 6 kPa.

The musician's lip plays a major role in sound production. It is pressed directly against the reed with a certain force controlled by the player. This force determines the height h_0 defined in Section 2. Guillemain et al. [91] measured the lip force with an FSR (Force Sensing Resistor) simultaneously with mouth and mouthpiece pressures. A saxophonist played a chromatic scale in the first register with legato. The lip force appeared to be fairly constant. When the musician separated the notes with his tongue, the lip force did not remain constant. As a result, the lip force was close to 0 before the attack of each note, as can be seen in Figure 21. These experimental values can also give indications to monitor the lip force applied by an artificial musician. However, measuring the lip force on the reed in this way is extremely complicated. As a matter of fact, it is necessary to stick a force sensor on the reed, which is likely to considerably hinder the musician's natural playing. Moreover, the FSR signal does not inform about the force value but gives only information about the force signal shape.

Secondly, such experiment setups can be used to study the reed behavior and to evaluate several of its parameters as equivalent stiffness, damping and mass. The first experiment in this way was conducted by Boutillon et al. [92]. Their aim was to compute saxophone reed stiffness from the measured input impedance of the instrument. In addition, the mouthpiece pressure was recorded while a musician played a note trying to keep a constant embouchure. It means that the musicians have to place the mouthpiece in the optimum mouth position to produce a stable sound.

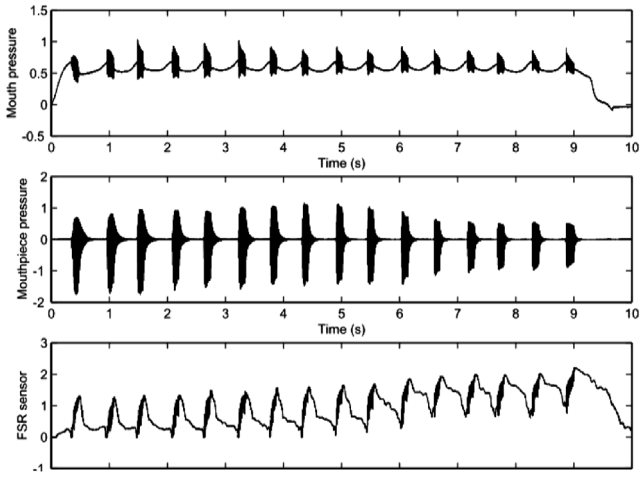

Figure 21. Mouth pressure, mouthpiece pressure and lip force of a saxophonist playing a chromatic scale. The notes are attacked [90].

This method proved to be promising as the computed stiffness values were of the same order of magnitude as previous results [57, 104]. However, the values were dependent on the measurement duration, the pitch and the dynamic of the note played. Then, Chatziioannou et al. [24] suggested an inverse modelling method to estimate clarinet reed parameters. They also planned to compute the reed stiffness, damping and effective surface as well. They recorded pressure and flow signals in a clarinet mouthpiece with three microphones. The parameters were calculated and optimized through a numerical procedure, taking into account a simplified lumped model intended to capture most of the dynamics of the reed-mouthpiece system. A 4-second-long single sustained note played by a clarinetist was recorded. Based on this recording, the proposed method provided numerical values for the reed parameters. Muñoz Arancón et al. [42] also designed a study to get an estimate of the reed parameters. Contrarily to Boutillon et al. [92] and Chatziioannou et al. [24], a direct method that does not require the whole instrument model was designed. The method enabled them to measure the pressure difference across the reed and the reed displacement by using an instrumented mouthpiece. The measured data was then used to estimate the parameters used in equation (11). They concluded that the most relevant model is the nonlinear oscillator containing nonlinear stiffness and damping, as illustrated by Figure 22. In addition, its estimations were the most accurate for small reed oscillations that do not generate reed beating. The typical values of all of these parameters are presented in Appendix A.

Last but not least, experiments performed in real-life situations with musicians, like those conducted by Petiot et al. [15], allow for the relationship between physical measurements and perceptual evaluations. In parallel to the perceptual study detailed in Section 3, a physical study with two saxophonists was conducted. Both the mouth and mouthpiece pressure were recorded thanks to an instrumented mouthpiece. The acoustic pressure at the bell of the saxophone was also measured. Two additional saxophonists performed arpeggios using the twenty reeds that were evaluated in the perceptual tests. Thirteen acoustical parameters extracted from the recorded signals were selected for further analysis. They highlighted that the threshold pressure which corresponds to the pressure in the mouth at the beginning of the permanent regime P_{Th} was highly correlated to five of these parameters as can be seen in Figure 23:

- Spectral Centroid *SC*,
- Odd-harmonic and Even-harmonic Spectral Centroid *OSC*, *ESC*,
- 2 Tristimuli *TR3* and *TR4* respectively defined as the ratio between the power of the higher harmonics from the 5th and the harmonics above 4000 Hz, and the total power of the harmonics.

They also showed that the acoustical parameters related to the mouth pressure were correlated with the timbre features.

4.3 Summary about physical reed measurement

The twelve families of experimental methods presented in Figure 12 for studying reeds have been detailed in this section. About 40 different experiments were carried out and some reached similar conclusions. In particular, microscopic observations of the reed cross-section enabled to consistently characterize the biological structure of the cane. Vascular bundles are inserted into the cell matrix called parenchyma. Depending on the growth conditions, fibers around the vascular bundles are more or less thick and numerous. The characteristics of these fibers impact the mechanical properties of the reed sample.

Mechanical measurements on the unmounted reed led to consistent results on the stiffness in static and dynamic conditions. Dynamic conditions showed that the first vibrational mode of the reed is far more present than the upper modes and slightly damped. These observations were carried out by different authors that obtained numerical values of the same order of magnitude for the eigenfrequencies [50, 70, 83]. The values are detailed in Appendix A.

As measurements on the unmounted reed does not give information about its behavior in playing conditions, some authors designed experimental protocols with both musicians and artificial musicians, with the reed linked to a mouthpiece and a lip. Such measurements can be used to observe, confirm and explain the results obtained in simulations. Moreover, the signals obtained (mouthpiece and mouth pressure, lip force and reed displacement) are representative of the reed behavior since the measurement are conducted under playing conditions.

However, the differences in the various test rigs designed and especially the different artificial lips led to incomparable situations between the different artificial musicians. The complexity of the instrumentation increases when a real musician takes the place of the artificial one. Because of sensors implemented in the mouthpiece, the clarinetists or saxophonists may play with an unusual embouchure that does

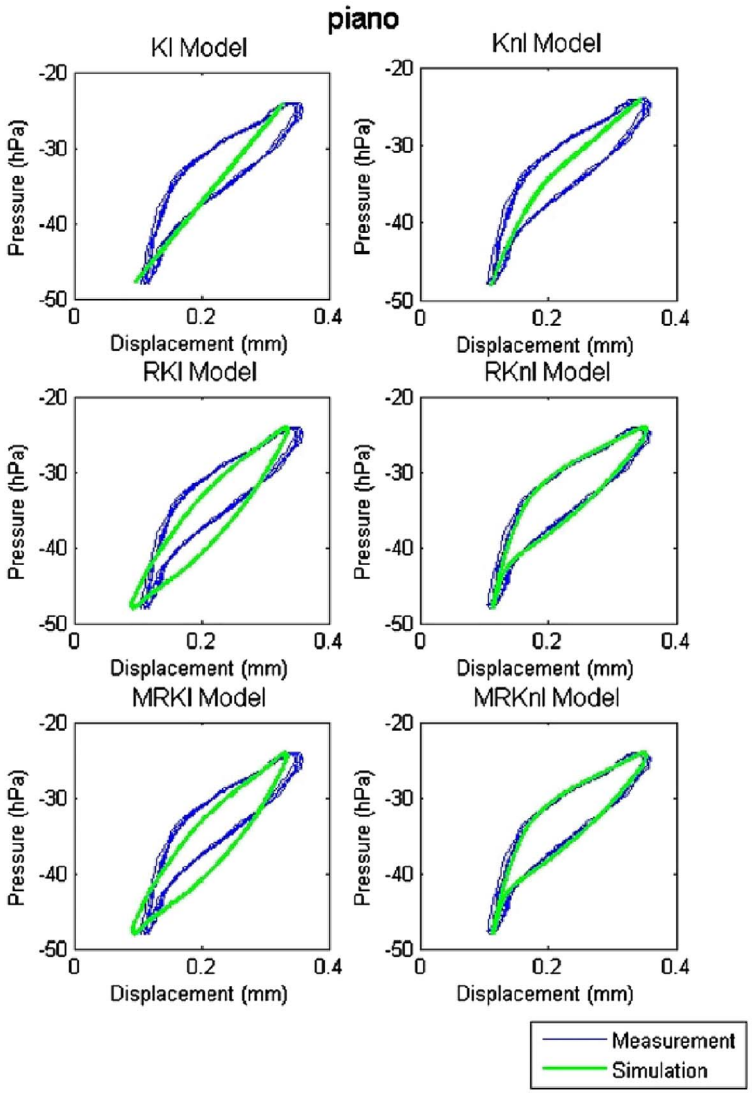

Figure 22. Pressure difference $p - P_M$ vs simulated (green) and measured (blue) displacement for the different physical models with small oscillations {*piano*} from Muñoz Arancón [14]. Left: linear models, right: nonlinear stiffness models. Up: models with stiffness only, middle: models with stiffness and damping, down: models with stiffness, damping and mass.

not reflect their playing habits. In addition, the environmental conditions of the reed, such as moisture and temperature, vary over time. Consequently, the physical reed parameters and the reed vibrational behavior may also vary, which makes the comparison between authors difficult.

5 Conclusions and perspectives

The present review aims at bringing together the numerous studies about single reeds and classifying them in three thematic categories.

A description of the reed's physical behavior and modeling techniques are covered in Section 2. Two families of models are used in the literature. The first family comprises the lumped element models. At a simple level of complexity, these models describe the reed as a simple stiffness, which enables the prediction of the threshold and closing pressures while knowing the opening at rest between the reed and the mouthpiece. These models can also take into account the dynamics of the reed and the contact force that relates the contact between the reed and the mouthpiece rails. In this case, the reed resonance frequency and the damping factor have an impact on the threshold pressure. The effective surface and the embouchure parameter (related to the opening at rest) have an impact on the regime selection and the playing frequency. The existence of a contact force explains the high-frequency components of the pressure signal due to the shock between the reed and the mouthpiece. The second family comprises the distributed models. These models make it possible to observe the fine behavior of reed vibration and to also estimate equivalent mechanical parameters (Young's modulus, ...) by comparing measurements and simulations.

Section 3 summarizes the studies about the perceptual assessment of reeds by musicians. As indicated in Table 1,

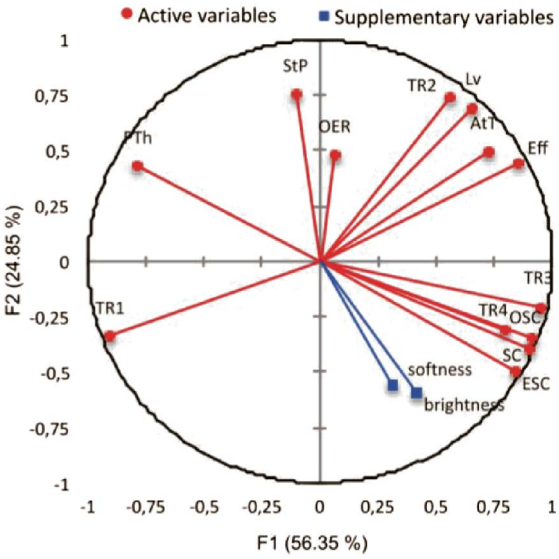

Figure 23. Principal component analysis on the 13 acoustical variables extracted by Petiot et al. [15].

they have been carried out using custom test protocols and methodologies. Consequently, the comparison of their observations is not straightforward, and the general conclusions that can eventually be drawn rely on numerous assumptions. One of the main goals of these perceptual studies was to explain the large perceptual differences that were observed between reeds that were considered identical. In order to establish a connection between the perceptual evaluations and physical parameters, physical measurements were conducted alongside each perceptual experiment.

Section 4 gives an overview of the numerous types of physical measurements that have been carried out on reeds. They were designed to measure biological or mechanical parameters, either in playing conditions or on the unmounted reed. The main relationships that were established between physical properties and perceptual features, especially regarding "overall quality" and "ease of playing", are recalled below.

Physical correlates of "global quality"

As stated in Section 3, there is no consensus on the exact denomination of "global quality". In any case, it seems that several studies have reached similar conclusions when comparing the biological parameters of "good" and "bad" reeds [10, 69, 79]. Firstly, a reed was considered to be "good" when constituted of wide and, above all, continuous fiber rings as shown in Figure 13. Secondly, a reed with a higher proportion of vascular bundle fibers than that of parenchyma cells was found better. Finally, the smaller the parenchyma cells and the thicker the parenchyma cell walls, the better the reed. In addition to this observation, Veselack [10] stated that fast-growing and immature canes present larger cells and thinner cell walls. She recommended to use two- or three-years grown canes to produce "good" reeds. Kolesik et al. [69] suspected that the environmental conditions of the crop has an effect on the quality of reeds. Especially, musicians reported that reeds made from harvested canes are slightly better than reeds from wild canes.

Some authors have hypothesized that the reed quality is related to the mechanical parameters describing its symmetry. Firstly, a "good" reed is supposed to be geometrically symmetrical. Groom [9] created a tool to control the reed symmetry and adjust it when needed. Secondly, according to Hanai [81] translated by Kawasaki et al. [79]: "The best quality reed has symmetry of the local rigidity in the blade tip". The measurements of the static reed tip stiffness carried out by Kemp et al. [67] and Gangl et al. [71] were in agreement with this assumption. Finally, other authors have also observed that reed quality is correlated with the symmetry of the first torsional mode [50, 70], which should contribute to the homogeneity of the reed tip movement. Despite these promising first results, no firm link has yet been established between reed symmetry and quality.

Physical correlates of "ease of playing"

Choosing "overall quality" for reed perceptual assessment led to major disagreements between musicians [14, 15]. Using "ease of playing" as a descriptor enabled more consistency in the assessments. While musicians may interpret the notion of quality differently, the notion of "ease of playing" is easier to understand and more universal.

Ease of playing can be physically quantified by the threshold pressure or the mean pressure in the musician's mouth inducing reed vibrations, as shown by Petiot et al. [15]. The reed compliance measured at the tip also proved to be correlated with "ease of playing" ($R = 0.74$). The measurements carried out by Gangl et al. [71] were in agreement with this conclusion.

Muñoz Arancón [14] found the "ease of playing" descriptor to be highly correlated ($R = 0.95$) with the timbre characteristic "brilliance", which is related to a high spectral centroid of the radiated pressure as shown by Petiot et al. [15] and confirmed by Gazengel et al. [66]. This can be explained by the fact that soft reeds may easily beat on the mouthpiece. As a consequence, the produced sound is likely to contain more higher harmonics.

Physical correlates of "intonation"

The intonation is related to the playing frequency of the instrument. According to the authors who studied the effect of reed parameters h_0, K_a, R_a, M_a, S_d on intonation, the most important is the effective surface S_d which is responsible for the reed volume velocity as shown by Coyle et al. [34]. However, simulation results obtained by Karkar et al. [29] showed that the embouchure parameter ζ, which is proportional to $\sqrt{\frac{h_0}{K_a}}$ has an impact on the frequency at the threshold, lowering the frequency (compared to the resonance frequency of the resonator) when increasing ζ.

The experimental work by Almeida et al. [105] demonstrated that mouth pressure and lip force affect the playing frequency. He showed that over the region of high pressure (up to 7 kPa) and high force (up to 3 kPa), the playing frequency increases both with increasing pressure and with

increasing lip force. This shows that the effective surface area S_d is decreased in both scenarios, except for low force values, and suggests that S_d depends on the generalized pressure defined in Section 2.2.2.

In his experimental and statistical approach, Taillard [56] hypothesized that intonation is related to the opening of the reed channel at rest h_{00} (without lip pressure). Statistical analysis performed on 40 reeds reveals that the playing frequency is inversely proportional to h_{00}. However, except for the work of Taillard [56], no other experimental study about intonation has been carried out on many reeds, so complementary investigations should be conducted to confirm this result.

Physical correlates of timbre

Obataya et al. [65] were interested in the timbral properties of reeds. In the perceptual tests they conducted, clarinetists played reeds that were subjected to chemical treatments, eliminating extractive substances. They found that the removal of extractives affected the softness and richness of the sounds, but that the reeds' ability to absorb glucose restored them. They finally concluded that the extractives play a major role in the acoustic properties of the reeds. Casadonte [13] argued that a symmetrical reed sounds better because it does not buzz. According to Taillard [27], the more symmetrical the reed, the more brilliant the sound. This is in line with the concept of buzz introduced by Casadonte since a reed sounds good if the timbre is "brilliant" instead of "buzzy".

Perspectives

Despite the numerous studies carried out on reeds and on reed's perceived quality in particular, formal conclusions on the subject remain insufficient. Further research is needed to expand our knowledge. Lastly, the authors feel that a number of directions should be investigated. First, the protocols for perceptual studies with musicians need to be improved so that intra and inter-musician agreements are better verified. In addition, it would be interesting to determine other indicators to describe the quality of a reed, putting aside the ease of playing, which seems to mainly dictate the musician's sensations.

Second, mechanical measurements on reeds have demonstrated their effectiveness, indicating that more study in this field is necessary. First, more precise methods for measuring static point stiffness on unmounted reeds could validate the importance of symmetry in reed stiffness. Second, using artificial musicians seems to be the most promising avenue for future research. Indeed, artificial musicians take into account the interaction between the reed and the mouthpiece and are more representative of real playing. Moreover, they offer a distinct advantage in the study of the reed in a playing context, providing a more robust and less complex approach than the use of real musicians. Numerous studies would be worth considering, and among them, the examination of the nonlinear part of the reed stiffness on the mouthpiece would be particularly interesting.

Conflicts of interest

The authors declare that they have no conflicts of interest.

Data availability statement

No new data were created or analyzed in this study.

References

1. L. Millot, C. Baumann: A proposal for a minimal model of free reeds, Acta Acustica united with Acustica 93, 1 (2007) 122–144.
2. M. Campbell, J. Gilbert, A. Myers: The science of brass instruments, Springer, Switzerland, 2021.
3. J.-P. Dalmont, B. Gazengel, J. Gilbert, J. Kergomard: Some aspects of tuning and clean intonation in reed instruments, Applied Acoustics 46, 1 (1995) 19–60.
4. C. Linnaeus: Systema naturae, vol. 1, Laurentii Salvii, Stockholm, 1758.
5. H.-C. Spatz, H. Beismann, F. Brüchert, A. Emanns, T. Speck: Biomechanics of the giant reed *Arundo donax*, Philosophical Transactions of the Royal Society of London. Series B: Biological Sciences 352, 1349 (1997) 1–10.
6. R.E. Perdue: *Arundo donax* – Source of musical reeds and industrial cellulose, Economic Botany 12, 4 (1958) 368–404.
7. A. Baines, A. Boult: Woodwind instruments and their history, Dover Publications, Mineola, NY, 1991.
8. V. Bucur: Handbook of materials for wind musical instruments, Springer, Switzerland, 2019.
9. N.E. Groom: An analysis of commercial single reed micrometers in the us and the development of a new manual single reed micrometer, PhD thesis, University of Maryland, 2020.
10. M.S.W. Veselack: Comparison of cell and tissue differences in good and unusable clarinet reeds, PhD thesis, Ball State University, 1979.
11. L.J. Intravaia, R.S. Resnick: A research study of a technique for adjusting clarinet reeds, Journal of Research in Music Education 16, 1 (1968) 45–58.
12. F. Berr: Traité complet de la clarinette à quatorze clefs: manuel indispensable aux personnes qui professent cet instrument et à celles qui l'étudient, E. Duverger, Paris, 1836.
13. D.J. Casadonte: The clarinet reed: an introduction to its biology, chemistry, and physics, PhD thesis, The Ohio State University, 1995.
14. A. Muñoz Arancón: New techniques for the characterisation of single reeds in playing conditions, PhD thesis, Le Mans Université, 2017.
15. J.-F. Petiot, P. Kersaudy, G.P. Scavone, S. McAdams, B. Gazengel: Investigation of the relationships between perceived qualities and sound parameters of saxophone reeds, Acta Acustica united with Acustica 103, 5 (2017) 812–829.
16. G. Legere: Oriented polymer reeds for musical instruments, July 11 2000. US Patent 6,087,571.
17. N.H. Fletcher, T. Rossing: The physics of musical instruments. 2nd edn., Springer, New York, NY, 2012.
18. A. Chaigne, J. Kergomard: Acoustics of musical instruments, Springer, New York, NY, 2016.
19. A. Chaigne, J. Kergomard: Acoustique des instruments de musique, Belin, Paris, 2008.
20. S.C. Thompson: The effect of the reed resonance on woodwind tone production, Journal of the Acoustical Society of America 66, 5 (1979) 1299–1307.

21. W. Li, A. Almeida, J. Smith, J. Wolfe: How clarinettists articulate: the effect of blowing pressure and tonguing on initial and final transients, Journal of the Acoustical Society of America 139, 2 (2016) 825–838.
22. M. Pàmies-Vilà, A. Hofmann, V. Chatziioannou: The influence of the vocal tract on the attack transients in clarinet playing, Journal of New Music Research 49, 2 (2020) 126–135.
23. T. Colinot, C. Vergez, P. Guillemain, J.-B. Doc: Multistability of saxophone oscillation regimes and its influence on sound production, Acta Acustica 5 (2021) 33.
24. V. Chatziioannou, M. Van Walstijn: Estimation of clarinet reed parameters by inverse modelling, Acta Acustica united with Acustica 98, 4 (2012) 629–639.
25. S. Bilbao, A. Torin, V. Chatziioannou: Numerical modeling of collisions in musical instruments, Acta Acustica united with Acustica 101, 1 (2015) 155–173.
26. J.-P. Dalmont, J. Gilbert, S. Ollivier: Nonlinear characteristics of single-reed instruments: quasistatic volume flow and reed opening measurements, Journal of the Acoustical Society of America 114, 4 (2003) 2253–2262.
27. P.-A. Taillard, F. Laloë, M. Gross, J.-P. Dalmont, J. Kergomard: Statistical estimation of mechanical parameters of clarinet reeds using experimental and numerical approaches, Acta Acustica united with Acustica 100, 3 (2014) 555–573.
28. M. van Walstijn, F. Avanzini: Modelling the mechanical response of the reed-mouthpiece-lip system of a clarinet. Part II: a lumped model approximation, Acta Acustica united with Acustica 93, 3 (2007) 435–446.
29. S. Karkar, C. Vergez, B. Cochelin: Oscillation threshold of a clarinet model: a numerical continuation approach, Journal of the Acoustical Society of America 131, 1 (2012) 698–707.
30. A. Hirschberg, R.W.A. Van de Laar, J.P. Marrou-Maurieres, A.P.J. Wijnands, H.J. Dane, S.G. Kruijswijk, A.J.M. Houtsma: A quasi-stationary model of air flow in the reed channel of single-reed woodwind instruments, Acta Acustica united with Acustica 70, 2 (1990) 146–154.
31. J.-P. Dalmont, J. Gilbert, J. Kergomard, S. Ollivier: An analytical prediction of the oscillation and extinction thresholds of a clarinet, Journal of the Acoustical Society of America 118, 5 (2005) 3294–3305.
32. B. Gazengel, J.-P. Dalmont, E. Hendrickx, M. Paquier, V. Koehl: Recherche d'indicateurs de qualité d'anches simples – partie 1: estimation des paramètres équivalents en régimes statique et quasi-statique, in: Proceedings of CFA2022, 16ème Congrès Français d'Acoustique, Marseille, France, 11–15 April, 2022.
33. J.-P. Dalmont, P. Guillemain, P.-A. Taillard: Influence of the reed flow on the intonation of the clarinet, in: Proceedings of Acoustics 2012 joint congress (11ème Congrès Français d'Acoustique – 2012 Annual IOA Meeting), Nantes, France, 23–27 April, 2012.
34. W.L. Coyle, P. Guillemain, J. Kergomard, J.-P. Dalmont: Predicting playing frequencies for clarinets: A comparison between numerical simulations and simplified analytical formulas, Journal of the Acoustical Society of America 138, 5 (2015) 2770–2781.
35. V. Chatziioannou, M. van Walstijn: Reed vibration modelling for woodwind instruments using a two-dimensional finite difference method approach, in: Proceedings of the International Symposium on Musical Acoustics (ISMA-07), Barcelona, Spain, 9–12 September, 2007.
36. E. Ducasse: A physical model of a single-reed wind instrument, including actions of the player, Computer Music Journal 27, 1 (2003) 59–70.
37. E. Ducasse: Modélisation et simulation dans le domaine temporel d'instruments à vent à anche simple en situation de jeu: méthodes et modèles, PhD thesis, Université du Maine, 2001.
38. V. Chatziioannou, A. Hofmann: Physics-based analysis of articulatory player actions in single-reed woodwind instruments, Acta Acustica united with Acustica 101, 2 (2015) 292–299.
39. K.H. Hunt, F.R. Erskine Crossley: Coefficient of restitution interpreted as damping in vibroimpact, Journal of Applied Mechanics 42, 2 (1975) 440–445.
40. S. Karkar, C. Vergez, B. Cochelin: Numerical tools for musical instruments acoustics: analysing nonlinear physical models using continuation of periodic solutions, in: Proceedings of Acoustics 2012 joint congress (11ème Congrès Français d'Acoustique – 2012 Annual IOA Meeting), Nantes, France, 23–27 April, 2012.
41. T. Colinot, L. Guillot, C. Vergez, P. Guillemain, J.-B. Doc, B. Cochelin: Influence of the "ghost reed" simplification on the bifurcation diagram of a saxophone model, Acta Acustica united with Acustica 105, 6 (2019) 1291–1294.
42. A. Muñoz Arancón, B. Gazengel, J.-P. Dalmont, E. Conan: Estimation of saxophone reed parameters during playing, Journal of the Acoustical Society of America 139, 5 (2016) 2754–2765.
43. V. Chatziioannou, S. Schmutzhard, M. Pàmies-Vilà, A. Hofmann: Investigating clarinet articulation using a physical model and an artificial blowing machine, Acta Acustica united with Acustica 105, 4 (2019) 682–694.
44. S.E. Stewart, W.J. Strong: Functional model of a simplified clarinet, Journal of the Acoustical Society of America 68, 1 (1980) 109–120.
45. S.D. Sommerfeldt, W.J. Strong: Simulation of a player-clarinet system, Journal of the Acoustical Society of America 83, 5 (1988) 1908–1918.
46. A. Ricardo da Silva, G.P. Scavone, M. van Walstijn: Numerical simulations of fluid-structure interactions in single-reed mouthpieces, Journal of the Acoustical Society of America 122, 3 (2007) 1798–1809.
47. F. Avanzini, M. van Walstijn: Modelling the mechanical response of the reed-mouthpiece-lip system of a clarinet. Part I: A one-dimensional distributed model, Acta Acustica united with Acustica 90, 3 (2004) 537–547.
48. V. Chatziioannou: Forward and inverse modelling of single-reed woodwind instruments with applications to digital sound synthesis, PhD thesis, Queen's University Belfast, 2010.
49. M.L. Facchinetti, X. Boutillon, A. Constantinescu: Numerical and experimental modal analysis of the reed and pipe of a clarinet, Journal of the Acoustical Society of America 113, 5 (2003) 2874–2883.
50. F. Pinard, B. Laine, H. Vach: Musical quality assessment of clarinet reeds using optical holography, Journal of the Acoustical Society of America 113, 3 (2003) 1736–1742.
51. T. Guimezanes: Etude expérimentale et numérique de l'anche de clarinette, PhD thesis, Université du Maine, 2008.
52. D. Roylance: Lecture notes in engineering viscoelasticity, Department of Materials Science and Engineering, Massachusetts Institute of Technology, Cambridge MA, 2001.
53. A.M.C. Valkering: Characterization of a clarinet mouthpiece. Technical Report R-1219-S, , Vakgroep Transportfysica – Eindhoven University of Technology, 1993.
54. T. Yoshinaga, H. Yokoyama, T. Shoji, A. Miki, A. Iida: Global numerical simulation of fluid-structure-acoustic interaction in a single-reed instrument, Journal of the Acoustical Society of America 149, 3 (2021) 1623–1632.

55. P.-A. Taillard: Theoretical and experimental study of the role of the reed in clarinet playing, PhD thesis, Le Mans Université, 2018.
56. C.J. Nederveen: Influence of reed motion on the resonance frequency of reed-blown wood-wind instruments, Journal of the Acoustical Society of America 45, 2 (1969) 513–514.
57. C.J. Nederveen: Acoustical aspects of woodwind instruments, PhD thesis, Northern Illinois University, 1998.
58. E. Ducasse: Modélisation d'instruments de musique pour la synthèse sonore: application aux instruments à vent, Le Journal de Physique Colloques 51, C2 (1990) C2–837.
59. J.-P. Dalmont, C. Frappé: Oscillation and extinction thresholds of the clarinet: comparison of analytical results and experiments, Journal of the Acoustical Society of America 122, 2 (2007) 1173–1179.
60. C. Fritz, S. Farner, J. Kergomard: Some aspects of the harmonic balance method applied to the clarinet, Applied acoustics 65, 12 (2004) 1155–1180.
61. E.A. Petersen, P. Guillemain, M. Jousserand: The dual influence of the reed resonance frequency and tonehole lattice cutoff frequency on sound production and radiation of a clarinet-like instrument, Journal of the Acoustical Society of America 151, 6 (2022) 3780–3791.
62. F. Fontana, S. Papetti, H. Järveläinen, F. Avanzini, B.L. Giordano: Perception of vibrotactile cues in musical performance, in: S. Papetti, C. Saitis (Eds.), Musical haptics, Springer, Switzerland, 2018, pp. 49–72.
63. A. Gaillard, V. Koehl, B. Gazengel: Link between stiffness symmetry and perceived quality of clarinet cane reeds, in: Proceedings of Forum Acusticum 2023, the 10th Convention of the European Acoustics Association, Turin, Italy, 11–15 September, 2023.
64. C. Fritz, D. Dubois: Perceptual evaluation of musical instruments: state of the art and methodology, Acta Acustica united with Acustica 101, 2 (2015) 369–381.
65. E. Obataya, M. Norimoto: Acoustic properties of a reed (*Arundo donax* L.) used for the vibrating plate of a clarinet, Journal of the Acoustical Society of America 106, 2 (1999) 1106–1110.
66. B. Gazengel, J.-P. Dalmont, J.-F. Petiot: Link between objective and subjective characterizations of Bb clarinet reeds, Applied Acoustics 106 (2016) 155–166.
67. C. Kemp, G.P. Scavone: Mechanical, anatomical and modeling techniques for alto saxophone reed evaluation and classification, Wood Science and Technology 54 (2020) 1677–1704.
68. S.C. Mukhopadhyay, G.S. Gupta, J.D. Woolley, S.N. Demidenko: Saxophone reed inspection employing planar electromagnetic sensors, IEEE Transactions on Instrumentation and Measurement 56, 6 (2007) 2492–2503.
69. P. Kolesik, A. Mills, M. Sedgley: Anatomical characteristics affecting the musical performance of clarinet reeds made from *Arundo donax* L. (Gramineae), Annals of Botany 81, 1 (1998) 151–155.
70. K. Stetson: Study of clarinet reeds using digital holography, Optical Engineering 53, 11 (2014) 112305–112305.
71. M. Gangl, A. Hofmann, A. Mayer: Comparison of characterization methods for B-flat clarinet reeds, in: Proceedings of the 7th AAAA Congress on Sound and Vibration, Ljubljana, Slovenia, 22–23 September, 2016.
72. V. Koehl, E. Hendrickx, M. Paquier, B. Gazengel, J.-P. Dalmont: Recherche d'indicateurs de qualité d'anches simples – partie 2: approche subjective, in: Proceedings of CFA2022, 16ème Congrès Français d'Acoustique, Marseille, France, 11–15 April, 2022.
73. S. McAdams, S. Winsberg, S. Donnadieu, G. De Soete, J. Krimphoff: Perceptual scaling of synthesized musical timbres: common dimensions, specificities, and latent subject classes, Psychological Research 58 (1995) 177–192.
74. R.A. Kendall, E.C. Carterette: Perceptual scaling of simultaneous wind instrument timbres, Music Perception 8, 4 (1991) 369–404.
75. A. Nykänen, Ö. Johansson, J. Lundberg, J. Berg: Modelling perceptual dimensions of saxophone sounds, Acta Acustica united with Acustica 95, 3 (2009) 539–549.
76. M. Barthet, P. Guillemain, R. Kronland-Martinet, S. Ystad: From clarinet control to timbre perception, Acta Acustica united with Acustica 96, 4 (2010) 678–689.
77. R. Viala: Personal communication, 2023, ITEMM (Intitut Technologique Européen des Métiers de la Musique).
78. V. Bucur: Traditional and new materials for the reeds of woodwind musical instruments, Wood Science and Technology 53, 5 (2019) 1157–1187.
79. M. Kawasaki, T. Nobuchi, Y. Nakafushi, M. Nose, M. Shibata, P. Li, M. Shiojiri: Structural observations and biomechanical measurements of clarinet reeds made from *Arundo donax*, Microscopy Research and Technique 80, 8 (2017) 959–968.
80. E. Ukshini, J.J.J. Dirckx: Longitudinal and transversal elasticity of natural and artificial materials for musical instrument reeds, Materials 13, 20 (2020) 4566.
81. K. Hanai: The measurement of the balance of the rigidity at the tip of a single reed – a reed with good acoustic quality has symmetrical rigidity between both sides and between the top and bottom surfaces, Pipers 351 (2010) 23–26 (in Japanese).
82. A. Calazans, A. Maurel-Pantel, F. Silva, G. Machado, C. Vergez, P. Sanchez, M. Rosenzweig, P. Eveno, M. Carron: Analyse microtomographique et vibroacoustique d'anches synthétiques pour saxophone, in: Proceedings of CFA2022, 16ème Congrès Français d'Acoustique, Marseille, France, 11–15 April, 2022.
83. P. Picart, J. Leval, F. Piquet, J.-P. Boileau, T. Guimezanes, J.-P. Dalmont: Study of the mechanical behaviour of a clarinet reed under forced and auto-oscillations with digital fresnel holography, Strain 46, 1 (2010) 89–100.
84. C.S. McGinnis, C. Gallagher: The mode of vibration of a clarinet reed, The Journal of the Acoustical Society of America 12, 4 (1941) 529–531.
85. E. Ukshini, J.J.J. Dirckx: Three-dimensional vibration patterns of alto saxophone reeds measured on different mouthpieces under mimicked realistic playing conditions, The Journal of the Acoustical Society of America 150, 5 (2021) 3730–3746.
86. T. Idogawa, T. Kobata, K. Komuro, M. Iwaki: Nonlinear vibrations in the air column of a clarinet artificially blown, The Journal of the Acoustical Society of America 93, 1 (1993) 540–551.
87. T. Kobata, T. Idogawa: Pressure in the mouthpiece, reed opening, and air-flow speed at the reed opening of a clarinet artificially blown, Journal of the Acoustical Society of Japan 14, 6 (1993) 417–428.
88. J. Backus: Vibrations of the reed and the air column in the clarinet, Journal of the Acoustical Society of America 33, 6 (1961) 806–809.
89. L. Fuks, J. Sundberg: Blowing pressures in bassoon, clarinet, oboe and saxophone, Acta Acustica united with Acustica 85, 2 (1999) 267–277.

90. M. Pàmies-Vilà, A. Hofmann, V. Chatziioannou: Analysis of tonguing and blowing actions during clarinet performance, Frontiers in Psychology 9 (2018) 617.
91. P. Guillemain, C. Vergez, D. Ferrand, A. Farcy: An instrumented saxophone mouthpiece and its use to understand how an experienced musician plays, Acta Acustica united with Acustica 96, 4 (2010) 622–634.
92. X. Boutillon, V. Gibiat: Evaluation of the acoustical stiffness of saxophone reeds under playing conditions by using the reactive power approach, Journal of the Acoustical Society of America 100, 2 (1996) 1178–1189.
93. C. Kemp: Characterisation of woodwind instrument reed (*Arundo donax* L) degradation and mechanical behaviour, PhD thesis, McGill University, 2019.
94. P. Smigielski: Holographie optique – Interférométrie holographique, Techniques de l'Ingénieur, 2001.
95. A. Muñoz Arancón, B. Gazengel, J.-P. Dalmont: Comparison of human and artificial playing of a single reed instrument, Acta Acustica united with Acustica 104, 6 (2018) 1104–1117.
96. C. Fritz, J. Wolfe: How do clarinet players adjust the resonances of their vocal tracts for different playing effects?, Journal of the Acoustical Society of America 118, 5 (2005) 3306–3315.
97. G.P. Scavone, A. Lefebvre, A. Ricardo da Silva: Measurement of vocal-tract influence during saxophone performance, Journal of the Acoustical Society of America 123, 4 (2008) 2391–2400.
98. J.M. Chen, J. Smith, J. Wolfe: Experienced saxophonists learn to tune their vocal tracts, Science 319, 5864 (2008) 776–776.
99. J.M. Chen, J. Smith, J. Wolfe: Pitch bending and glissandi on the clarinet: Roles of the vocal tract and partial tone hole closure, Journal of the Acoustical Society of America 126, 3 (2009) 1511–1520.
100. J.M. Chen, J. Smith, J. Wolfe: Saxophonists tune vocal tract resonances in advanced performance techniques, Journal of the Acoustical Society of America 129, 1 (2011) 415–426.
101. S.M. Lulich, S. Charles, B. Lulich: The relation between tongue shape and pitch in clarinet playing using ultrasound measurements, Journal of the Acoustical Society of America 141, 3 (2017) 1759–1768.
102. W. Li, A. Almeida, J. Smith, J. Wolfe: Tongue, lip and breath interactions in clarinet playing: a study using a playing machine, in: Proceedings of the 21st International Congress on Sound and Vibration, ICSV21, Beijing, China, 13–17 July, 2014.
103. E. Pillinger: The effects of design on the tone and response of clarinet mouthpieces, PhD thesis, London Guildhall University, 2000.
104. J. Gilbert: Etude des instruments de musique à anche simple: extension de la méthode d'équilibrage harmonique, rôle de l'inharmonicité des résonances, mesure des grandeurs d'entrée, PhD thesis, Université du Maine, 1991.
105. A. Almeida, D. George, J. Smith, J. Wolfe: The clarinet: How blowing pressure, lip force, lip position and reed "hardness" affect pitch, sound level, and spectrum, Journal of the Acoustical Society of America 134, 3 (2013) 2247–2255.
106. Reeds technical elements. Available at https://vandoren.fr/en/reeds-technical-elements/ (accessed 02-20-2024).
107. W.E. Worman: Self-sustained nonlinear oscillations of medium amplitude in clarinet-like systems, PhD thesis, Case Western Reserve University, 1971.

Appendix A

Reed parameter values

This appendix gives the numerical values associated to different materials (cane, synthetic) and different instruments (clarinet, saxophone). The geometry of the reed is defined in Figure A1.

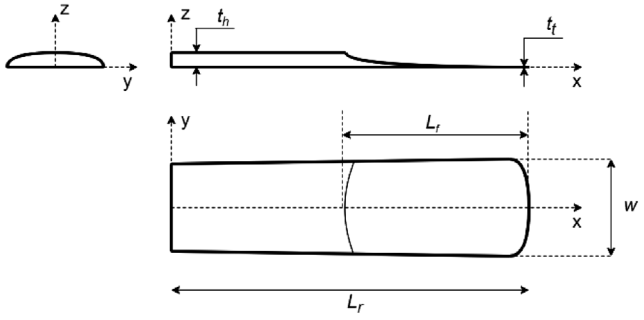

Figure A1. Geometry of the reed (x: longitudinal, y: transversal, z: radial, L_r: reed length, L_f: free or vibrating length, w: width, t_t: tip thickness, t_h: heel thickness).

A.1 Geometrical parameters

The geometrical parameters of clarinet reeds are given in Table A1.

A.2 Structural mechanical parameters

The structural mechanical parameters used in publications dedicated to the numerical modelling of the reed in 1-D or 2-D (see Sects. 2.2.3 and 2.2.4) are given in Table A2.

Guimezanes [51] shows that the mechanical parameters depend on the longitudinal position on the reed (x axis) as given in Figure A2 (with $L_f = 35$ mm) and Table A3.

A.3 Equivalent mechanical parameters

A.3.1 Reed alone

To our knowledge, Nederveen [56] conducted the first measurements on reeds alone using a distributed static load. He reported the values given in the Table A4 for different instruments. The measurements have been done on a reed of medium hardness that is free to move.

Table A5 gives the point-stiffness measured more recently on reeds alone (without lip or mouthpiece) using a static load by three different authors. In these experiments, the force and the displacement are measured at the same location.

Table A6 gives the parameters of a reed alone measured with a dynamic acoustic excitation.

A.3.2 Reed, lip and mouthpiece

Static measurement. Quasi-static Measurements performed by Taillard in [55] (Fig. 4.11) for clarinet reeds mounted on a mouthpiece (with a lip) give an estimation of the reed compliance of 1 mm^2 kPa^{-1}. Assuming the width of the reed is $w = 13.15$ mm leads to a compliance of 0.07 mm kPa^{-1} (stiffness equal to $1.43 \cdot 10^7$ N m^{-3}).

Table A1. Geometrical parameters of clarinet reeds.

Dimensions	Value (mm)	Reference
Width w	13.15	[49]
Total length L_r	67.5	[49]
Free or vibrating length L_f	34.1	[49]
Tip thickness t_t	[0.09–0.11]	[106]
	0.15	[78]
Heel thickness t_h	[2.8–3.25]	[106]

Table A2. Order of magnitude of mechanical clarinet reed parameters E_x (longitudinal Young's modulus), E_y (transverse Young's modulus), G_{xy}, G_{xz} and G_{yz} shear moduli, Poisson's ratio ν_x and ν_y, cane density ρ_r.

Material	Cane					Fibracell
Reference	[49, 50]	[51]	[80]	[48]	[27]	[37]
ρ_r (kg m^{-3})	450	520	500	500	520	500
E_x (GPa)	10	3 to 9.5	5	10	14	10
E_y (GPa)	0.4	0.2 to 0.5	0.5	0.4		1
G_{xz} (GPa)	1.3	0.6 to 0.87		1.3	1.1	0.5
$G_{xz} = G_{Yz}$ (GPa)					1.2	0.3
ν_x (–)	0.22	0.22		0.22		0.35
ν_y (–)				0.08		
η (s)				$6 \cdot 10^{-6}$		

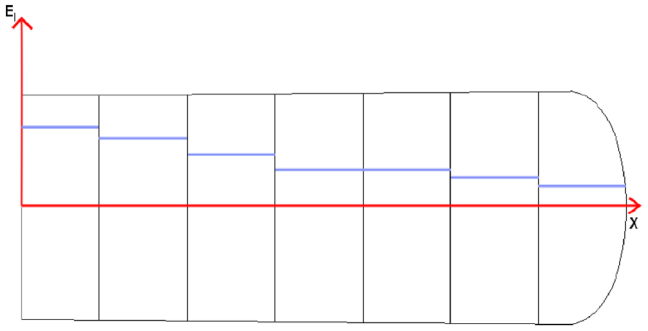

Figure A2. View of the reed sectors used for defining different mechanical parameters given in Table A3 [51].

Table A3. Optimal parameters proposed by Guimezanes [51] in order to fit experimental and simulated frequency responses for one clarinet cane reed.

x (mm)	$x = 5$	$x = 10$	$x = 15$	$x = 20$	$x = 25$	$x = 30$	$x = 35$
E_x (MPa)	9500	8000	6200	4300	4000	4800	3000
E_y (MPa)	500	500	250	250	250	200	200
G_{xy} (MPa)	600	600	600	600	1100	870	870

Table A4. Compliance and stiffness of different instrument reeds as measured by Nederveen [56].

Instrument	Clarinet	Saxophone		
		Tenor	Alto	Soprano
Compliance $\frac{1}{K_a}$ (m^3 N^{-1})	10^{-7}	$3 \cdot 10^{-7}$	$1.2 \cdot 10^{-7}$	10^{-7}
Stiffness K_a (N m^{-3})	10^7	$3.33 \cdot 10^6$	$8.33 \cdot 10^6$	10^7

Table A5. Order of magnitude of equivalent clarinet reed point-stiffness for the reed alone. L_f is the free length (between the clamping and the reed tip), and x_t is the distance between the reed tip and the measurement points. The minimum value of K_p is measured on the sides of the reed, whereas the maximum value of K_p is measured in the middle.

Reference	[67]		[63]	
L_f (mm)	38.25		30	
x_t (mm)	1	5	3	10
K_p (N mm^{-1})	$\in$ [0.5–1]	$\in$ [1.5–2.5]	$\in$ [0.5–1]	$\in$ [3–7]

Table A6. Order of magnitude of equivalent clarinet reed parameters (resonance frequency, quality factor, compliance) of reed alone. L_f is defined in Figure A1, x_t is the distance between the reed tip and the sensor, f_1 is the resonance frequency, Q_1 is the quality factor, C_1 is the equivalent compliance of the first vibration mode and $K_1 = \frac{1}{C_1}$ is the equivalent stiffness.

Reference	[66]	[50]	[70]
Mounting	On bench	On mouthpiece	
L_f (mm)	30		
x_t (mm)	2		
f_1 (Hz)	[1890–2270]	$\in$ [2140–2440] (dry) $\in$[1530–1890] (wet)	2300 (dry) 2060 (wet)
Q_1 (–)	$\in$ [30–50]		
C_1 (m Pa^{-1})	$\in$ [15–40] 10^{-9}		
K_1 (N m^{-3})	$\in$ [2.5–6.7] 10^7		

Table A7. Order of magnitude of equivalent reed parameters (mass, damping, stiffness, resonance frequency, quality factor) of reed + lip system in simulated or real playing situation.

Instrument	Clarinet			Tenor saxophone
Reference	[107]	[28]	[24]	[42]
Conditions	Measurements	Simulation	Measurements	
Effective area $S_r = S_d$ (m^2)		[3–8] 10^{-5}	$1.77 \cdot 10^{-4}$	
Equivalent stiffness K_a (N m^{-3})	$1.24 \cdot 10^7$	[7–21] 10^6	$1.24 \cdot 10^7$	$4.8 \cdot 10^6$
Equivalent mass M_a (kg m^{-2})	0.0231	0.05	0.056	0.269
Resonance frequency (Hz)	3687.4	[1883–3262]	2368.3	672
Equivalent resistance R_a (kg s^{-1} m^{-2})	67	145	25.4	$1 \cdot 10^3$
Equivalent damping g (s^{-1})	2900	2900	453	3717
Equivalent quality factor Q_r	8	[4.1–7]	32.8	1.13
Equivalent damping factor q_r	0.125	[0.14–0.24]	0.03	0.88
Nonlinear stiffness k_c (N m^{-4})			$3.7 \cdot 10^{11}$	$7 \cdot 10^{11}$

Real playing situation. Table A7 contains equivalent geometrical area ($S_d = S_r$) and equivalent mechanical parameters (mass M_a, damping R_a or equivalent, stiffness, and nonlinear stiffness as given in Sect. 2.2.2) estimated from real instrument measurements or from numerical simulations.

A.4 Pressures

The blowing pressures for the clarinet are $P_m \in$ [2.0–5.9] kPa, for the saxophone $P_m \in$ [1.3–8.3] kPa [88]. Sound level in tenor sax mouthpiece for pianissimo level is 146 dB SPL and 162 dB SPL for *forte* [42].

Appendix B

Chatziioannou model

Figure B1 shows the physical variables as defined by Chatziioannou [24].

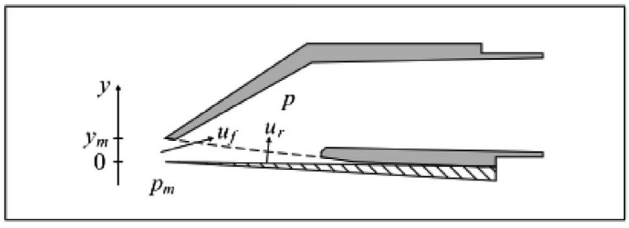

Figure B1. Definition of variables by Chatziioannou.

The motion of reed is written

$$m\ddot{y} + m\gamma\dot{y} + ky + k_c\lfloor y - y_c\rfloor^{\alpha}(1 + r_c\dot{y}) = S_r p_\Delta, \qquad \text{(B1)}$$

with y the reed tip opening, $p_\Delta = p_m - p$. The parameters related to the contact are k_c (contact stiffness), α (collision exponent), r_c (contact damping). $\lfloor x \rfloor$ can be written $\lfloor x \rfloor = \frac{x+|x|}{2}$ (activation for $x \geq 0$).

Appendix C

Our model

Figure C1 shows the physical variables as defined by Gaillard et al.

The reed tip opening is written here $h_0 - h$ so that the equivalence between the two models is $y = h_0 - h$. Introducing $h_0 - h$ in equation (B1) leads to

$$-m\ddot{h} - m\gamma\dot{h} + k(h_0 - h) + k_c\lfloor h_0 - h - y_c\rfloor^{\alpha}(1 - r_c\dot{h}) = S_r p_\Delta, \qquad \text{(C1)}$$

which can be written

$$-M_a\ddot{h} - R_a\dot{h} + K_a(h_0 - h) + K_c\lfloor h_c - h\rfloor^{\alpha}(1 - r_c\dot{h}) = p_\Delta, \qquad \text{(C2)}$$

with $M_a = \frac{m}{S_r}$, $R_a = \frac{m\gamma}{S_r}$, $K_a = \frac{k}{S_r}$, $K_c = \frac{k_c}{S_r}$, $h_c = h_0 - y_c$. This leads to

$$M_a\ddot{h} + R_a\dot{h} + K_a(h - h_0) - K_c\lfloor h_c - h\rfloor^{\alpha}(1 - r_c\dot{h}) = -p_\Delta, \qquad \text{(C3)}$$

This can be written

$$M_a\ddot{h} + R_a\dot{h} + K_a(h - h_0) = -p_\Delta + F_c, \qquad \text{(C4)}$$

with

$$F_c = K_c\lfloor h_c - h\rfloor^{\alpha}(1 - r_c\dot{h}). \qquad \text{(C4)}$$

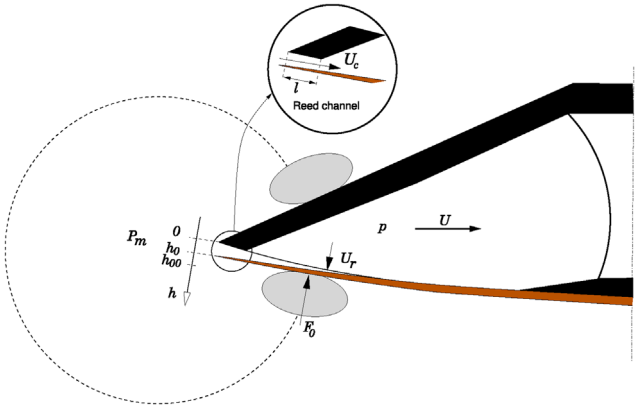

Figure C1. Definition of variables by Gaillard et al.

Cite this article as: Gaillard A. Koehl V. & Gazengel B. 2024. Theoretical and experimental studies about single cane reeds: a review. Acta Acustica, **8**, 63. https://doi.org/10.1051/aacus/2024050.